

### **RESEARCH ARTICLE**

# Caenorhabditis elegans establishes germline versus soma by balancing inherited histone methylation

Brandon S. Carpenter<sup>1</sup>, Teresa W. Lee<sup>1</sup>, Caroline F. Plott<sup>2</sup>, Juan D. Rodriguez<sup>1</sup>, Jovan S. Brockett<sup>3</sup>, Dexter A. Myrick<sup>1</sup> and David J. Katz<sup>1,\*</sup>

#### **ABSTRACT**

Formation of a zygote is coupled with extensive epigenetic reprogramming to enable appropriate inheritance of histone methylation and prevent developmental delays. In Caenorhabditis elegans, this reprogramming is mediated by the H3K4me2 demethylase SPR-5 and the H3K9 methyltransferase, MET-2. In contrast, the H3K36 methyltransferase MES-4 maintains H3K36me2/3 at germline genes between generations to facilitate re-establishment of the germline. To determine whether the MES-4 germline inheritance pathway antagonizes spr-5; met-2 reprogramming, we examined the interaction between these two pathways. We found that the developmental delay of spr-5; met-2 mutant progeny is associated with ectopic H3K36me3 and the ectopic expression of MES-4-targeted germline genes in somatic tissues. Furthermore, the developmental delay is dependent upon MES-4 and the H3K4 methyltransferase, SET-2. We propose that MES-4 prevents crucial germline genes from being repressed by antagonizing maternal spr-5; met-2 reprogramming. Thus, the balance of inherited histone modifications is necessary to distinguish germline versus soma and prevent developmental delay.

This article has an associated 'The people behind the papers' interview.

KEY WORDS: Histone methylation, Developmental delay, Maternal reprogramming, Transgenerational inheritance, Epigenetics, Caenorhabditis elegans

#### INTRODUCTION

In multicellular organisms, developmental cell fate decisions are established by tightly controlled spatial and temporal gene expression (Frum and Ralston, 2015; Gregor et al., 2014; Maduro, 2010). One key control of gene expression is through the regulation of histone methylation, which controls gene expression by regulating the accessibility of DNA to transcription factors and RNA polymerase (Burton and Torres-Padilla, 2014; Hirabayashi and Gotoh, 2010; Jambhekar et al., 2019). For example, methylation of either lysine 4 or 36 on histone 3 (H3K4me and H3K36me) is associated with active transcription, whereas methylation of lysine 9 on the same histone (H3K9me) is commonly associated with transcriptional repression (Bannister et al., 2005; Barski et al., 2007; Bernstein et al., 2002, 2005). In addition, histone methylation on the

<sup>1</sup>Department of Cell Biology, Emory University School of Medicine, Atlanta GA 30322, USA. <sup>2</sup>Johns Hopkins University School of Medicine, Baltimore MD 21205, USA. <sup>3</sup>Department of Biology, Oglethorpe University, Atlanta GA 30319, USA.

\*Author for correspondence (djkatz@emory.edu)

**(D)** B.S.C., 0000-0001-9939-1926; T.W.L., 0000-0002-0149-5389; D.J.K., 0000-0002-3040-1142

Handling Editor: Swathi Arur Received 31 August 2020; Accepted 4 January 2021 N-terminal tails of histone proteins can be heritable through cell division, and across generations via both the sperm and oocyte. Inheritance of histone methylation across generations results in the maintenance of transcriptional states, which can affect the development and survivability of the offspring (Gaydos et al., 2014; Jambhekar et al., 2019; Kaneshiro et al., 2019; Öst et al., 2014; Siklenka et al., 2015; Tabuchi et al., 2018).

Histone methylation is dynamically regulated by the specific and tightly controlled activity of histone modifying enzymes (Morgan and Shilatifard, 2020), which regulate gene expression during development (Jambhekar et al., 2019). For example, mono- and dimethylation of lysine 4 on histone H3 (H3K4me1/2) are removed by the demethylase LSD1 (also known as KDM1A; Shi et al., 2004, 2005). In the nematode Caenorhabditis elegans, populations of mutants lacking the LSD1 ortholog, SPR-5, become increasingly sterile over ~30 generations (Katz et al., 2009). Failure to erase H3K4me2 at fertilization between generations in spr-5 mutants correlates with an accumulation of H3K4me2 and spermatogenesis gene expression across 30 generations, which leads to increasing sterility (Katz et al., 2009). These data demonstrate that H3K4me2 can function as an epigenetic transcriptional memory through cell divisions and across generations. In addition to transgenerational sterility, the accumulation of H3K4me2 in spr-5 mutants is associated with meiotic defects, increased longevity and a synergistic increase in sterility in an rbr-2 mutant background (Alvares et al., 2014; Greer et al., 2016; Nottke et al., 2011). These transgenerational phenotypes provide further evidence that H3K4 methylation functions as a transcriptional memory across generations.

More recently, it was demonstrated that SPR-5 synergizes with the H3K9me2 methyltransferase MET-2 to regulate maternal epigenetic reprogramming (Greer et al., 2014; Kerr et al., 2014). Progeny of mutants lacking both SPR-5 and MET-2 suffer from developmental delay and become completely sterile in a single generation. These phenotypes are associated with synergistic increases in both H3K4me2 and candidate germline gene expression in somatic tissues (Kerr et al., 2014). Together, this work supports a model in which SPR-5 and MET-2 are maternally deposited into the oocyte, where they reprogram histone methylation to prevent inherited defects. Consistent with H3K9 methylation functioning together with the erasure of H3K4me2, loss of the histone demethylase JMJD-2, which can demethylate H3K9, partially suppresses the transgenerational sterility caused by loss of SPR-5 (Greer et al., 2014).

Following fertilization, the *C. elegans* embryo separates germline versus somatic lineages progressively through a series of asymmetric divisions (Strome, 2005). To accomplish this, transcription factors coordinate with multiple histone modifications. For example, maternal deposition of PIE-1, a germline-specific protein that asymmetrically segregates into germline blastomeres (P lineage cells), maintains the fate of germ cells by inhibiting RNA polymerase II (POL-II)

elongation and preventing the ectopic expression of somatic genes (Batchelder et al., 1999; Mello et al., 1992; Seydoux et al., 1996). In the absence of transcription in the germline, the maternally provided H3K36me2/3 methyltransferase MES-4 binds to a subset of germline genes that were previously expressed in the parental germline (Furuhashi et al., 2010; Rechtsteiner et al., 2010). These germline genes are recognized by MES-4 via H3K36me2/3 that was added in the parental germline by the transcription-coupled H3K36me2/3 methyltransferase MET-1 (Kreher et al., 2018). MES-4 maintains H3K36me2/3 at these genes in the early embryo in a transcriptionally independent manner. Without maternally deposited MES-4, the germline cannot properly proliferate and animals are sterile (Capowski et al., 1991; Garvin et al., 1998). For the remainder of this study, we will refer to the genes that are bound by MES-4 and which maintain H3K36me3 throughout embryogenesis in a transcription-independent fashion, as 'MES-4 germline genes'. In addition, the process through which the MES-4 germline inheritance system maintains these genes for re-activation in the offspring will be referred to as 'bookmarking'.

MES-4 bookmarking is antagonized in somatic tissues by transcriptional repressors and chromatin remodelers. For example, loss of the transcriptional repressors LIN-15B and LIN-35 at high temperatures leads to larval arrest (Petrella et al., 2011). This larval arrest can be suppressed by removing the MES-4 germline inheritance system (Petrella et al., 2011). Removing the MES-4 inheritance system also suppresses the somatic expression of germline genes in lin-35 mutants (Wang et al., 2005). Similar to LIN-15B and LIN-35, loss of the chromatin remodelers MEP-1 and LET-418 causes somatic expression of germline genes and larval arrest (Unhavaithaya et al., 2002). The somatic expression of germline genes and larval arrest in mep-1 and let-418 mutants is also dependent upon the MES-4 germline inheritance system (Unhavaithaya et al., 2002). Together, these findings demonstrate that transcriptional repressors antagonize H3K36 bookmarking by MES-4 in somatic tissues.

Recently, the repressive histone modification H3K9me2 has been implicated in the somatic repression of germline genes (Rechtsteiner et al., 2019). Some germline genes have H3K9me2 enrichment at their promoters in somatic tissues, suggesting that H3K9me2 mediates their repression somatically (Rechtsteiner et al., 2019). Loss of LIN-15B reduces this enrichment of H3K9me2 leading to the ectopic accumulation of H3K36me3 at gene bodies in somatic tissues (Rechtsteiner et al., 2019). This raises the possibility that LIN-15B may repress MES-4 germline inheritance in somatic tissues in part through the repressive histone modification H3K9me2. However, this model remains to be tested.

Despite the extensive knowledge of the transcriptional repression pathways that somatically antagonize the MES-4 germline inheritance system, it remains unclear why germline genes are bookmarked by H3K36 in the embryo. To address this gap, we examined somatic development in progeny deficient in SPR-5 and MET-2 maternal reprogramming. Our previous work suggests that maternal spr-5; met-2 reprogramming prevents the transgenerational inheritance of H3K4me2 by erasing this mark and coupling it to the acquisition of H3K9me2 between generations (Kerr et al., 2014). Here, we show that H3K36me3 ectopically accumulates at MES-4 germline genes in the somatic tissues of spr-5; met-2 double-mutant progeny (hereafter referred to as *spr-5*; *met-2* progeny), and this accumulation correlates with the ectopic expression of these genes. In addition, we find that both the developmental delay and the ectopic expression of germline genes is rescued by RNAi-mediated depletion of MES-4 activity. These data provide evidence that the ectopic expression of MES-4targeted germline genes in somatic tissues leads to developmental delay at the larval stage. In addition, we demonstrate that the severe developmental delay of *spr-5*; *met-2* progeny is rescued by the loss of the H3K4 methyltransferase SET-2. This finding suggests that the ectopic maintenance of the MES-4 germline inheritance system in *spr-5*; *met-2* progeny is driven by the inheritance of H3K4 methylation. Finally, by demonstrating that loss of maternal *spr-5*; *met-2* reprogramming leads to expression of MES-4 germline genes in somatic tissues, our data suggest that H3K36 methylation bookmarking functions to antagonize *spr-5*; *met-2* maternal reprogramming. Thus, we propose that *C. elegans* balances three different histone modifications to distinguish between the competing fates of soma and germline.

#### **RESULTS**

### Loss of spr-5 and met-2 causes a severe developmental delay

Previous observations from our lab have indicated that progeny from spr-5; met-2 mutants may develop abnormally (Kerr et al., 2014). To further characterize this phenotype, we synchronized embryos laid by wild-type (N2), spr-5, met-2 and spr-5; met-2 mutant hermaphrodites and monitored their development from hatching to adults. By 72 h, all wild-type progeny (469/469), most of the spr-5 progeny (363/385) and many of met-2 progeny (386/ 450) were fertile adults (Fig. 1A-C,E; Fig. S1A-C). In contrast, spr-5; met-2 progeny displayed a severe developmental delay, with none of the progeny (0/463) reaching adulthood by 72 h (Fig. 1D,E; Fig. S1D). The majority of spr-5; met-2 progeny (371/463) resembled L2 larvae at 72 h, while a smaller percentage of the population developed to later larval stages (42/463) (Table S1). This larval delay occurs despite embryogenesis being accelerated in spr-5; met-2 progeny versus wild type (Fig. S2). This indicates that the larval delay is not just due to a general delay in all cell divisions. By seven days post synchronized lay, a small number of spr-5; met-2 progeny (35/876) developed into adults and the majority (31/35) of these adults displayed protruding vulva (Fig. S1E-G; Kerr et al., 2014). All 35 of the *spr-5*; *met-2* mutant progeny that developed to adulthood were sterile.

# MES-4 germline genes are ectopically expressed in *spr-5;* met-2 mutant soma

Previously we have shown that H3K4me2 is synergistically increased in spr-5; met-2 progeny compared with spr-5 and met-2 single mutant progeny, and that this increase in H3K4me2 correlates with a synergistic increase in candidate germline gene expression in somatic tissues (Kerr et al., 2014). To test the extent to which germline genes are ectopically expressed in somatic tissues, we examined somatic expression genome-wide. To do this, we performed RNA-seq on spr-5; met-2 L1 progeny compared with wild-type L1 progeny. We chose to perform this analysis on L1 larvae because this stage immediately precedes the L2 larval delay that we observed in spr-5; met-2 progeny (see Fig. 1D). In addition, L1 larvae are composed of 550 somatic cells and two germ cells. Therefore, L1 larvae are primarily composed of somatic tissue. As a control, we also performed RNA-seq on L1 progeny from spr-5 and met-2 single mutants that were isolated from early generation animals within the first five generations. These generations are well before the onset of sterility that we previously reported (Katz et al., 2009; Kerr et al., 2014).

We identified 778 differentially expressed transcripts in *spr-5; met-2* progeny compared with wild type (Figs S3A,B, S4C,F; Table S4), many of which also overlap with genes differentially expressed in *spr-5* (113/343, hypergeometric test, *P*-value <6.88e-

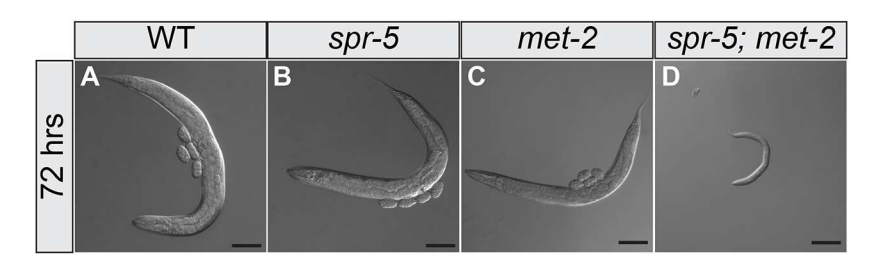
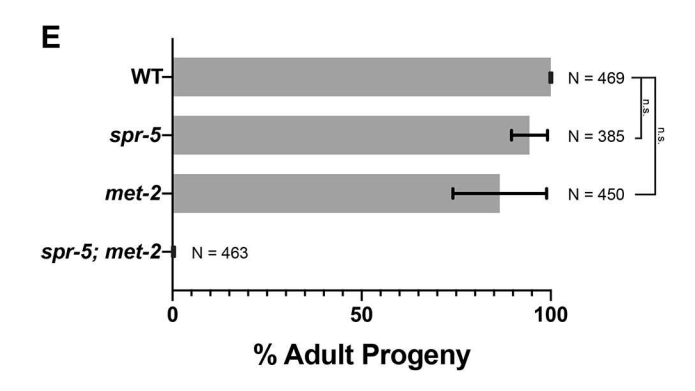


Fig. 1. spr-5; met-2 mutants display severe developmental delay. (A-D) Representative 10× differential interference contrast (DIC) images of wild-type (A), spr-5 (B), met-2 (C) and spr-5; met-2 progeny (D) 72 h post synchronized lay. (E) Percentage of wild-type, spr-5, met-2 and spr-5; met-2 progeny that reached the adult stage (% Adult Progeny) by 72 h post synchronized lay. Data are mean±s.d. from three experiments. N, the total number of progeny 20-25 hermaphrodites scored over three experiments. n.s. indicates a P-value >0.05 (two-tailed unpaired t-test). Scale bars: 100 μm.



75) and met-2 single mutants (159/413, hypergeometric test, P-value<7.15e-119) compared with wild type (Figs S3A,B, S4A,B,D,E; Tables S2,S3). Gene Ontology (GO) analysis did not identify any categories of genes misexpressed in the spr-5 or met-2 single mutants. However, the GO analysis revealed that genes differentially expressed in *spr-5*; *met-2* progeny were significantly enriched (based on Combined Score; Chen et al., 2013) for biological processes and cellular components characteristic of the germline; including meiosis, P-granules and negative regulation of the cell cycle (Fig. S3C,D). Many of these germline functioning genes are expressed in the germline of the parental generation, bound by the H3K36 methyltransferase MES-4 in the early embryo, and marked by H3K36me2/3, independent of POL-II (referred to as MES-4 germline genes) (Rechtsteiner et al., 2010). As a result, we were interested in the potential overlap between genes that are misregulated in *spr-5*; *met-2* progeny and MES-4 germline genes.

Rechtsteiner and colleagues identified approximately 200 MES-4 germline genes (Rechtsteiner et al., 2010). We reasoned that the absence of SPR-5 and MET-2 reprogramming may cause these germline genes to be aberrantly targeted by MES-4 in the soma, leading to ectopic expression. To investigate this possibility, we examined the overlap between differentially expressed genes in spr-5; met-2 L1 progeny and MES-4 germline genes. Out of 196 MES-4 germline genes, 34 overlapped with genes upregulated in spr-5; met-2 progeny compared with wild type (Fig. S5A; hypergeometric test, P-value<6.44e-20), whereas zero overlapped with genes downregulated in spr-5; met-2 progeny compared with wild type (Fig. S5B). In addition, when we compared the log2 fold change (FC) in expression of all of the MES-4 germline genes in spr-5, met-2 and spr-5; met-2 mutant progeny compared with wild type, we observed that 108 of the MES-4 germline genes were synergistically increased in spr-5; met-2 progeny compared with single mutant progeny (Fig. S5C; Table S6).

During this initial RNA-seq analysis we had to genotype every *spr-5; met-2* L1 because the balancer chromosome (a chromosome that blocks homologous recombination) that was available did not completely balance *spr-5*. As a result, the RNA-seq was performed

using a low-input sequencing technique (see Materials and Methods). However, during the course of the experiments, a new balancer became available that completely balanced spr-5. This enabled us to repeat the spr-5; met-2 RNA-seq experiments using standard amounts of RNA. In the repeat spr-5; met-2 RNA-seq experiment (referred to as repeat experiment two), we identified significantly more differentially expressed genes compared with wild type (4223 versus 778 in the initial low-input analysis, Fig. S6A,B). However, despite the larger number of differentially expressed genes, MES-4 germline genes remained similarly enriched. Out of 196 MES-4 germline genes, 112 overlapped with genes up-in spr-5; met-2 progeny compared with wild type (Fig. 2A; hypergeometric test, P-value<1.20e-54; Fig. S6C,D; Table S5), while only two overlapped with genes downregulated in spr-5: met-2 progeny compared with wild type (Fig. 2B). We also compared the log2FC in expression of all of the MES-4 germline genes in spr-5; met-2 mutant progeny compared with wild type. This analysis revealed that the MES-4 germline genes in repeat experiment two were similarly overexpressed in spr-5; met-2 progeny compared with wild type (Fig. 2C; Fig. S6E; Table S6). Interestingly, although MES-4 germline genes were enriched in both spr-5; met-2 RNA-seq experiments, there were some differences in the specific MES-4 germline genes that were overexpressed, and the extent to which they were overexpressed (Fig. S6E; Table S6).

# smFISH confirmation of MES-4 germline gene expression in spr-5; met-2 mutant soma

To confirm that MES-4 germline genes are somatically expressed in *spr-5; met-2* L1 progeny, we performed single molecule fluorescent *in situ* hybridization (smFISH) on two MES-4 germline targets, *htp-1* and *cpb-1* (Fig. 3). Both of these genes were amongst the genes that were ectopically expressed in *spr-5; met-2* L1 progeny compared with wild-type L1 progeny. In wild-type L1 larvae, *htp-1* (Fig. 3A-C, insets) and *cpb-1* (Fig. 3G-I, insets) were restricted to the two primordial germ cells, Z2 and Z3, which go on to form the entire adult germline. This confirms that these transcripts are

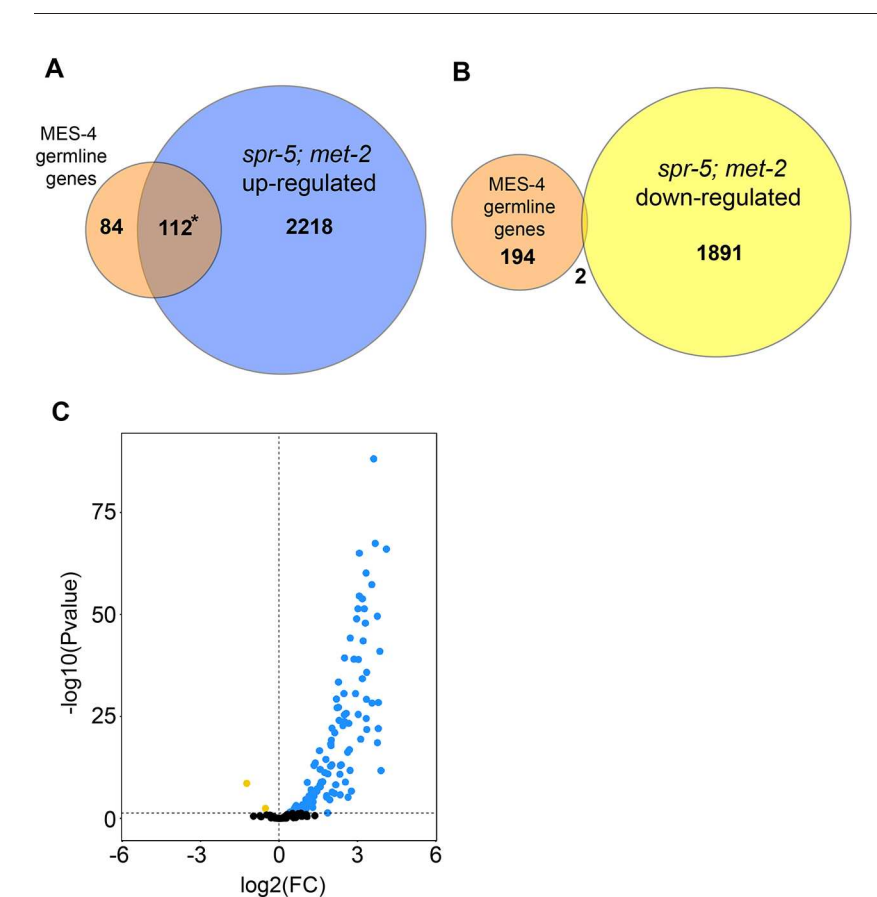


Fig. 2. MES-4 germline genes are ectopically expressed in *spr-5; met-2* mutant soma in RNA-seq repeat experiment two. (A,B) Overlap between MES-4 germline genes and genes upregulated (A) and downregulated (B) in *spr-5; met-2* L1 progeny (first repeat experiment shown in Figs S3-S6). Significant over-enrichment in A was determined by the hypergeometric test (\*P-value <1.20E-54). (C) Volcano plot of log2 fold changes (FC) of 196 MES-4 germline gene expression (*x*-axis) in *spr-5; met-2* L1 progeny compared with wild-type L1 progeny by statistical significance (-Log<sub>10</sub> P-value; *y*-axis). Yellow dots represent significantly upregulated genes determined by DESEQ2 analysis (see Materials and Methods). *P*-adi<0.05 (Wald test).

confined to the germline as expected. In contrast, in *spr-5; met-2* progeny, *htp-1* was ectopically expressed throughout the soma (Fig. 3D-F). This expression pattern is similar to what we observed with the ubiquitously expressed subunit of RNA polymerase II, *ama-1* (Fig. S7), which was unchanged in our RNA-seq analysis. *cpb-1* was also ectopically expressed in *spr-5; met-2* progeny, though the ectopic expression was not as ubiquitous as *htp-1* (Fig. 3J-L). To determine whether *htp-1* is also ectopically expressed in earlier embryonic stages, we performed smFISH on the embryos of *spr-5; met-2* progeny. In wild-type embryos, *htp-1* is restricted to Z2 and Z3 at the 200+ cell stage (Fig. S8A-C). In contrast, in *spr-5; met-2* progeny at the 200+ cell stage we detected the ectopic expression of *htp-1* (Fig. S8D-F), indicating that *htp-1* is ectopically expressed before the L1 larval stage.

# MES-4 germline genes maintain ectopic H3K36me3 in *spr-5;* met-2 mutants

To test whether MES-4 germline genes that are ectopically expressed in the soma of *spr-5; met-2* progeny also ectopically maintain H3K36me3, we performed H3K36me3 chromatin immunoprecipitation (ChIP)-seq. MES-4 germline genes have low levels of H3K36me3 in wild-type L1 progeny. However, compared with wild-type L1 progeny, *spr-5; met-2* L1 progeny displayed increased enrichment for H3K36me3 across gene bodies at MES-4 germline genes (Fig. 4A-C; Fig. S9A-C,W,X). For example, the MES-4 germline genes *cpb-1*, *T05B9.1*, *Y18D10A.11*, *fbxa-101* and *htp-1* that are ectopically expressed in our RNA-seq analysis, showed increased levels of H3K36me3 in *spr-5; met-2* progeny (Fig. 4O-S; Fig. S9O-S) compared with wild-type progeny (Fig. 4G-K; Fig. S9G-K). As a control, we examined H3K36me3 enrichment at genes that are not affected in *spr-5; met-2* progeny.

These control genes include: *ceh-13*, a gene enriched in hypodermal and ventral nerve chord in L1 progeny (Fig. 4L,T; Fig. S9L,T), *ama-1*, a subunit of RNA polymerase II that is expressed ubiquitously (Fig. 4M,U; Fig. S9M,U), and *act-1*, which encodes a ubiquitously expressed actin-related protein (Fig. 4N,V; Fig. S9N,V). Each of these control genes displayed similar H3K36me3 enrichment in both *spr-5*; *met-2* and wild-type L1 progeny (compare Fig. 4T-V and Fig. S9T-V with Fig. 4L-N and Fig. S9L-N, respectively). In addition, we found that the enrichment in H3K36me3 is substantially reduced when we examine H3K36me3 across all germline genes (Fig. 4D-F; Fig. S9D-F). This suggests that the enrichment in H3K36me3 is confined to the subset of germline genes that are MES-4 targets.

# MES-4 germline genes display H3K9me2 at their promoter peaks

Recent work has discovered that some germline-specific genes contain H3K9me2 peaks at their promoters in wild-type L1 progeny (Rechtsteiner et al., 2019). This finding implicates H3K9me2 enrichment at promoters of germline genes as being a crucial component for repressing germline genes in somatic tissues. If SPR-5 and MET-2 are functioning to prevent MES-4 germline genes from being ectopically expressed in somatic tissues, we would expect MES-4 germline genes that are ectopically expressed in the somatic tissues of *spr-5; met-2* progeny to normally continue to be targeted by H3K9 methylation in these tissues. To examine this possibility, we re-analyzed L1 stage H3K9me2 Chip-seq data from Rechsteiner et al. (2019). This re-analysis showed that many of the MES-4 germline genes were enriched for H3K9me2 at their promoters (Fig. S10A), including the majority of MES-4 germline genes that were ectopically expressed in the soma of *spr-5; met-2* 

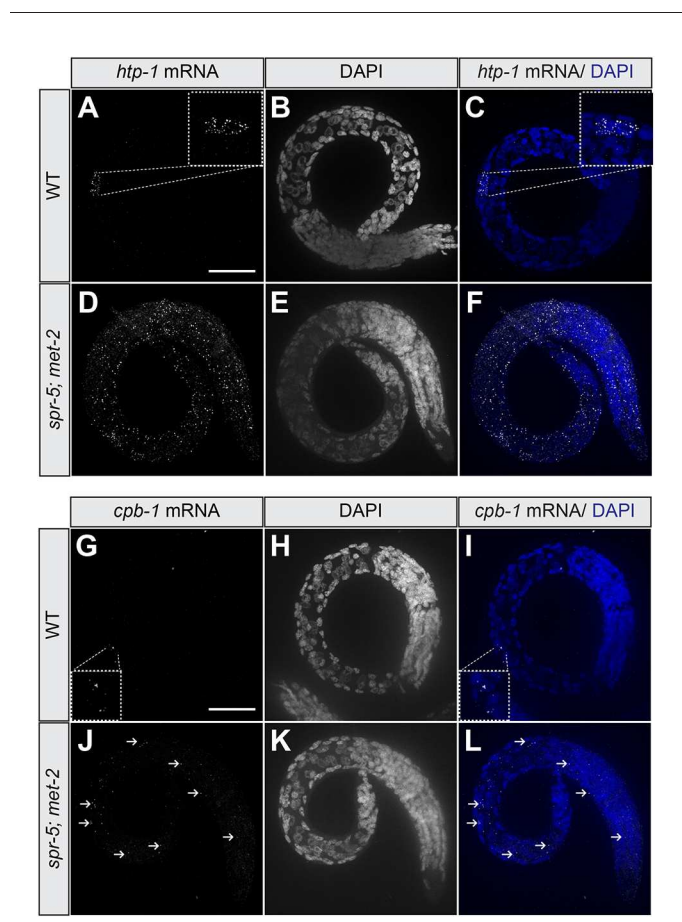


Fig. 3. spr-5; met-2 L1 progeny ectopically express MES-4 germline genes in multiple somatic tissues. (A-L) Representative  $40\times$  smFISH images of htp-1 (A,C,D,F) and cpb-1 (G,I,J,L) endogenous mRNAs in wild-type (A-C,G-I) and spr-5; met-2 (D-F,J-L) L1 progeny. DAPI was used as a nuclear marker. Insets show high magnification images of the germ cells, Z2 and Z3, in wild-type L1 progeny. Arrows (J,L) denote ectopic cpb-1 mRNA foci in somatic cells. Scale bars:  $40~\mu m$ .

progeny (Fig. S10B). For example, the MES-4 germline genes *cpb-1*, *T05B9.1*, *Y18D10A.11*, *fbxa-101* and *htp-1* that were misexpressed somatically and accumulated ectopic H3K36me3 in the somatic tissues of *spr-5*; *met-2* progeny, had H3K9me2 peaks at their promoters (Fig. S10C-G). In contrast, our control genes *ceh-13*, *ama-1* and *act-1* that were not misexpressed were also not enriched for H3K9me2 at their promoters (Fig. S10H-J).

# Knocking down MES-4 rescues ectopic expression of germline genes in *spr-5*; *met-2* mutant soma

To test whether the ectopic expression of MES-4 germline genes in *spr-5; met-2* progeny is dependent on the ectopic H3K36me3, we examined whether the expression of these genes was dependent upon MES-4. We performed quantitative real-time PCR (qRT-PCR) on L1 progeny from *spr-5; met-2* hermaphrodites fed control (L4440) RNAi versus *mes-4* RNAi (Fig. 5). For this analysis, we selected candidate MES-4 germline genes that were ectopically expressed and displayed an ectopic H3K36me3 peak in *spr-5; met-2* L1 progeny compared with wild-type L1 progeny. Consistent with our RNA-seq analysis, all nine of the candidate MES-4 germline genes that we examined were ectopically expressed >2-fold in *spr-5; met-2* L1 progeny compared with wild-type L1 progeny (Fig. 5). Strikingly, the ectopic expression of the nine MES-4 candidate germline genes was dependent upon MES-4. Nine out of

nine of these genes were significantly decreased in L1 progeny from spr-5; met-2 hermaphrodites treated with mes-4 RNAi (Fig. 5; twotailed unpaired t-test, P-value <0.001), and all but one (T05B9.1) were reduced to levels that were similar to wild-type L1 progeny. During this analysis, expression levels were normalized to the ubiquitously expressed large subunit of RNA polymerase (AMA-1), which was unaffected. This suggests that the effects of mes-4 RNAi are confined to the ectopically expressed MES-4 germline genes. In addition, to confirm that the reduced expression of MES-4 germline genes in spr-5; met-2 progeny treated with mes-4 RNAi was due to the elimination of the ectopic expression of MES-4 germline genes, we performed smFISH on the two MES-4 germline targets, htp-1 and cpb-1, in L1 progeny from spr-5; met-2 hermaphrodites fed control (L4440) RNAi versus mes-4 RNAi (Fig. S11). mes-4 RNAi eliminated the ectopic smFISH signal. This demonstrated that the expression of these two MES-4 germline targets in somatic tissues was dependent upon MES-4.

#### MES-4 is not ectopically expressed in spr-5; met-2 progeny

It is possible that SPR-5 and MET-2 may target MES-4 germline genes directly. Alternatively, SPR-5 and MET-2 could target the *mes-4* locus, resulting in indirect effects on MES-4 germline genes. To distinguish between these possibilities, we determined whether MES-4 is ectopically expressed in *spr-5*; *met-2* progeny by examining the expression of a *mes-4::GFP* transgene in these animals. We do not detect any ectopic expression of MES-4 in *spr-5*; *met-2* progeny (Fig. S12). This suggests that SPR-5 and MET-2 do not function indirectly by repressing *mes-4*.

# Knocking down MES-4 rescues developmental delay in *spr-5; met-2* progeny

To test whether the developmental delay phenotype that we observed in *spr-5*; *met-2* progeny is also dependent on the ectopic expression of MES-4 germline genes, we fed spr-5; met-2 hermaphrodites mes-4 RNAi and monitored their progeny for 72 h after a synchronized lay. If the developmental delay is dependent upon the ectopic expression of MES-4 germline genes, it should be suppressed when this ectopic expression is eliminated via mes-4 RNAi. By 72 h, all of the wild-type progeny from hermaphrodites fed either L4440 control (1089/1089) or mes-4 (1102/1102) RNAi were adults (Fig. 6A,B,G). Also, consistent with our previous observations, all but one of the spr-5; met-2 mutant progeny (729/730) from hermaphrodites fed control RNAi remained in the L2-L3 larval stages (Fig. 6D,G). In contrast, most of spr-5; met-2 progeny (569/618) from hermaphrodites fed mes-4 RNAi developed to adults (Fig. 6E,G; unpaired *t*-test, *P*<0.0001). Though, as expected, these animals remained sterile owing to the mes-4 RNAi preventing any germline formation.

# Knocking down SET-2 rescues *spr-5; met-2* developmental delay

If the developmental delay of *spr-5*; *met-2* mutants is caused by ectopic inheritance of H3K4me2 driving the expression of MES-4 germline genes in somatic tissues, we would expect the developmental delay of *spr-5*; *met-2* progeny to be dependent upon the H3K4 methyltransferase SET-2. To test this, we monitored the development of progeny of *spr-5*; *met-2* hermaphrodites fed *set-2* RNAi for 72 h after a synchronized lay. Identical to wild-type progeny from hermaphrodites fed control RNAi, *set-2* RNAi had no effect on the development of wild-type animals, as all of the wild-type progeny from hermaphrodites fed *set-2* RNAi developed to

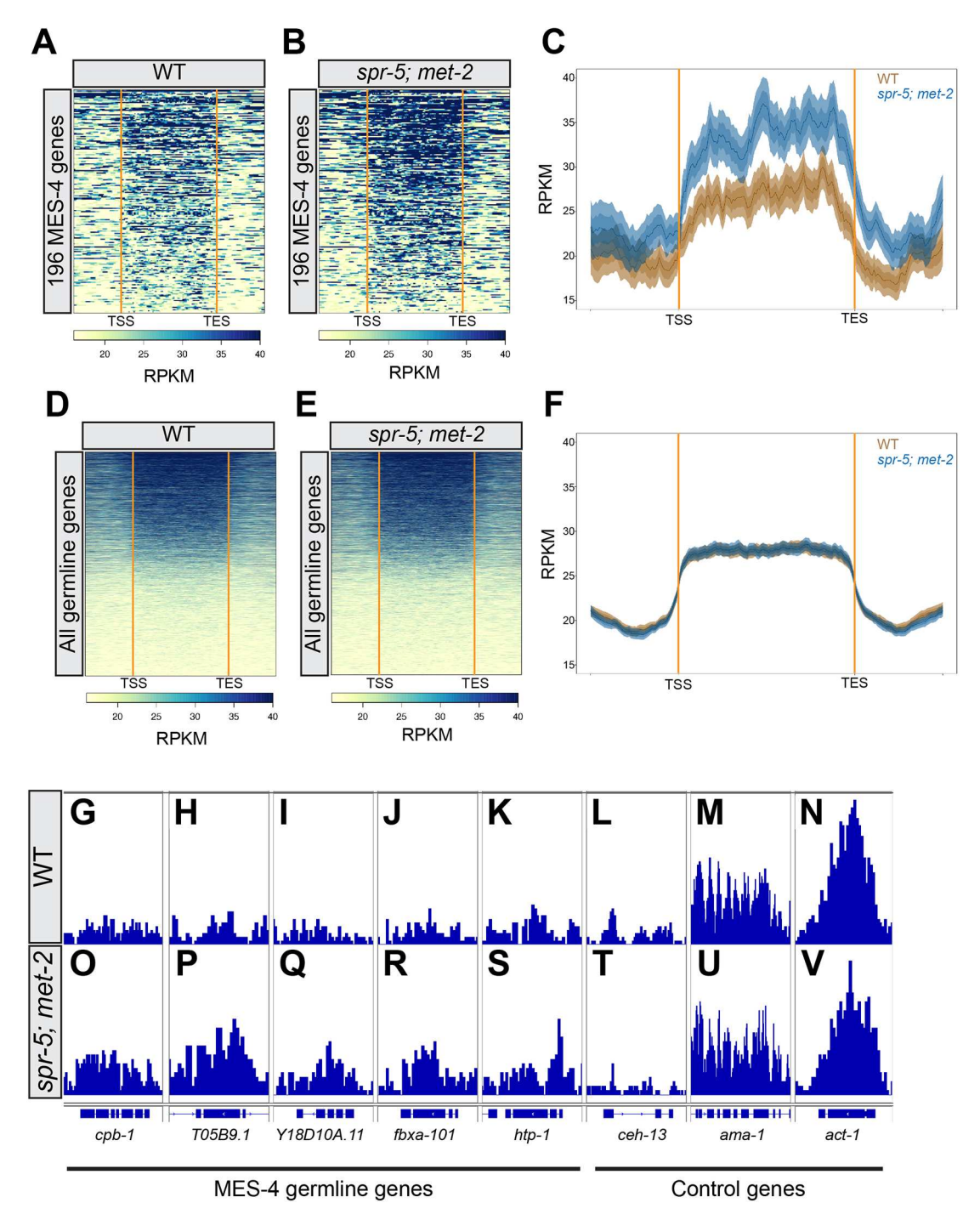


Fig. 4. MES-4 germline genes display ectopic H3K36me3 in *spr-5; met-2* L1 progeny. (A,B) Heatmap of H3K36me3 ChIP-seq reads normalized to RPKM over the gene bodies of 196 MES-4 germline genes in wild-type (A) versus *spr-5; met-2* (B) L1 progeny (second replicate in Fig. S9). (C) Plot profile corresponding to heatmaps in A (wild type, brown) and (B) (*spr-5; met-2*, blue). (D,E) Heatmap of H3K36me3 ChIP-seq reads normalized to RPKM over the gene bodies of all germline genes in wild-type (D) versus *spr-5; met-2* (E) L1 progeny. (F) Plot profile corresponding to heatmaps in D (wild type, brown) and E (*spr-5; met-2*, blue). Gene bodies were pseudoscaled to 1 kb with 500 bp borders separated by orange bars that represent the transcriptional start site (TSS) and transcriptional end site (TES). (G-V) Integrative genome viewer (IGV) image of H3K36me3 ChIP-seq reads normalized to RPKM at MES-4 germline genes (G-K,O-S) and control genes (L-N,T-V) in wild-type (G-N) versus *spr-5; met-2* (O-V) L1 progeny. RPKM IGV windows were scaled between 0 and 202 RPKM for all genes.

adults by 72 h (1114/1114) (Fig. 6C,G). However, in contrast to *spr-5; met-2* progeny fed control RNAi that were developmentally delayed, most of the progeny from *spr-5; met-2* hermaphrodites fed *set-2* RNAi developed to adults (347/384) (Fig. 6F,G; unpaired *t*-test, *P*<0.0001).

# spr-5; met-2 progeny acquire transgene silencing in somatic tissues

The somatic expression of MES-4 germline genes involved in germline transgene silencing (Figs S4C and S5C) raises the possibility that the somatic tissues in *spr-5*; *met-2* progeny may

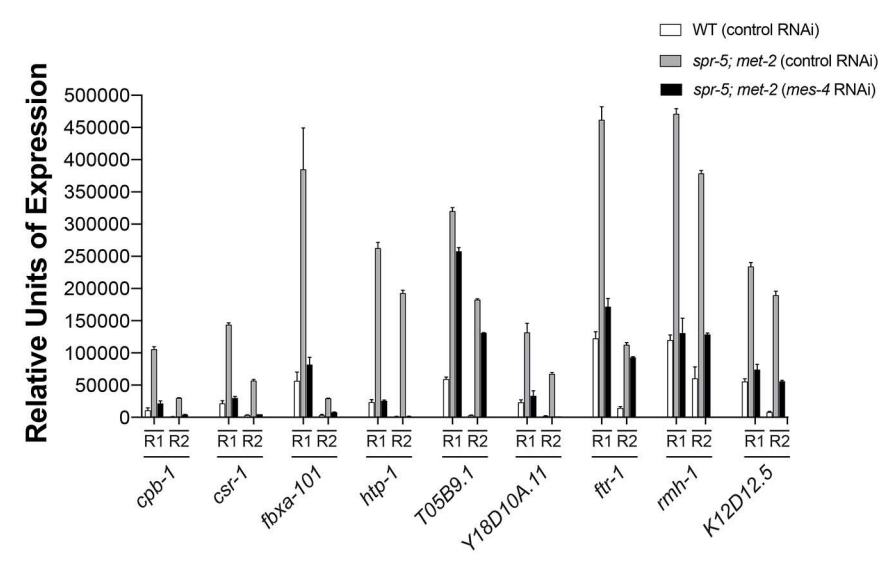


Fig. 5. Knocking down MES-4 rescues ectopic expression of MES-4 germline genes in spr-5; met-2 L1 progeny. Quantitative RT-PCR showing the relative units of expression for nine MES-4 germline genes (cpb-1, csr-1, fbxa-101, htp-1, T05B9.1, Y18D10A.11, ftr-1, rmh-1, K12D12.5) in L1 progeny of spr-5; met-2 hermaphrodites fed either control L4440 RNAi (gray bars) or mes-4 RNAi (black bars) versus wild type fed control L4440 RNAi (white bars). Relative units of expression from two biological replicates (R1 and R2) were calculated for each gene by averaging triplicate RT-PCR reactions and normalizing to a control gene, ama-1 (see Table S11 for raw values from RT-PCR analysis). Data are mean±s.e.m. for triplicate RT-PCR reactions. For all nine genes, mes-4 RNAi significantly reduced the relative expression of spr-5; met-2 compared with spr-5; met-2 fed L4440 control RNAi. P<0.001 (twotailed unpaired t-test). See Table S12 for a summary of how these genes performed across the assays performed for this study.

**MES-4 Germline Genes** 

acquire the ability to silence transgenes, a function normally restricted to germline cells. To test this, we examined the somatic expression of an extrachromosomal multicopy *let-858* transgene that is normally silenced in the germline by both transcriptional and posttranscriptional germline silencing mechanisms (Kelly and Fire, 1998). This analysis was performed in *spr-5; met-2* mutant L2 larvae that were undergoing developmental delay. In wild type, most of the L2 progeny (117/132) expressed ubiquitous high levels of LET-858::GFP throughout the entire soma (Fig. 7A,B,K),

whereas the remaining progeny (15/132) expressed what we described as a 'faint' level of expression (Fig. 7C,D,K). In contrast, almost none of the *spr-5; met-2* L2 progeny (2/87) displayed a high level of transgene expression comparable with the high level seen in most wild-type progeny (Fig. 7E,F,K). Instead, the majority of *spr-5; met-2* progeny (64/87) had faint LET-858:: GFP expression that is comparable with the faint expression observed in wild-type progeny (Fig. 7G,H,K). The remaining 21 *spr-5; met-2* progeny had no LET-858:: GFP expression. Because

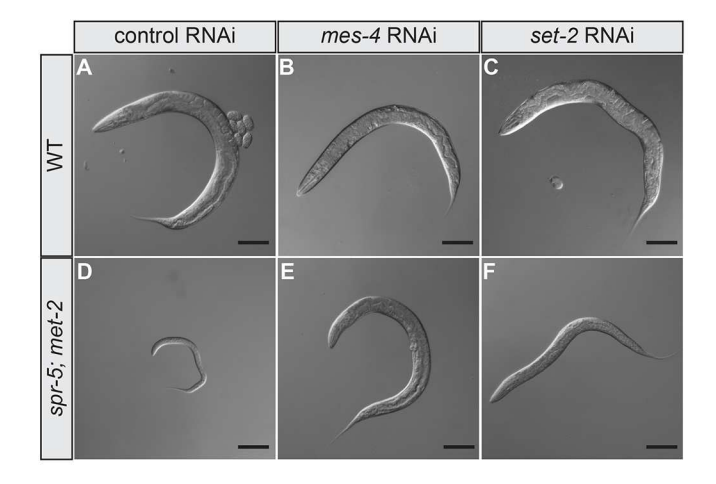
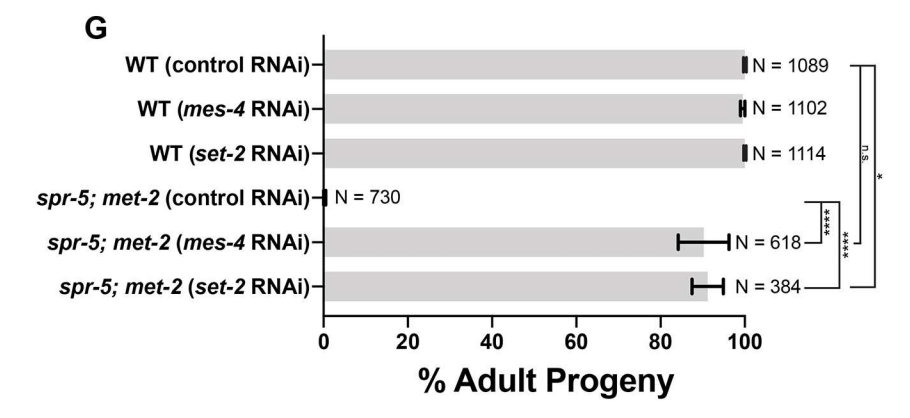
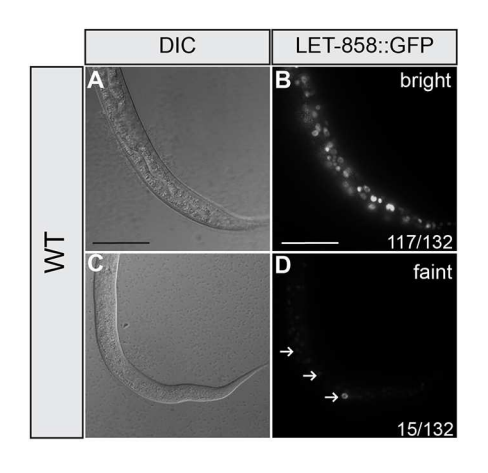
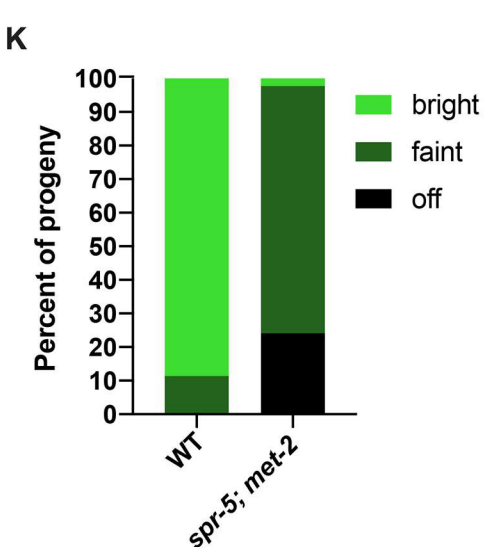


Fig. 6. Knocking down MES-4 rescues developmental delay in *spr-5; met-2* progeny. (A-F) DIC images of wild-type (A-C) or *spr-5; met-2* (E-F) progeny from hermaphrodite parents treated with control (L4440 vector only) RNAi (A,D), *mes-4* RNAi (B,E) or *set-2* RNAi (C,F) 72 h post synchronized lay. (G) Quantification of the number of progeny (represented as % Adult Progeny) from A-F that made it to adults by 72 h. Data are mean± s.d. from two or three experiments. N represents the total number of progeny from 30-40 hermaphrodites scored across independent experiments. \**P*<0.05, \*\*\*\*\**P*<0.0001 (two-tailed unpaired *t*-test). n.s. represents *P*>0.05. Scale bars: 100 µm.







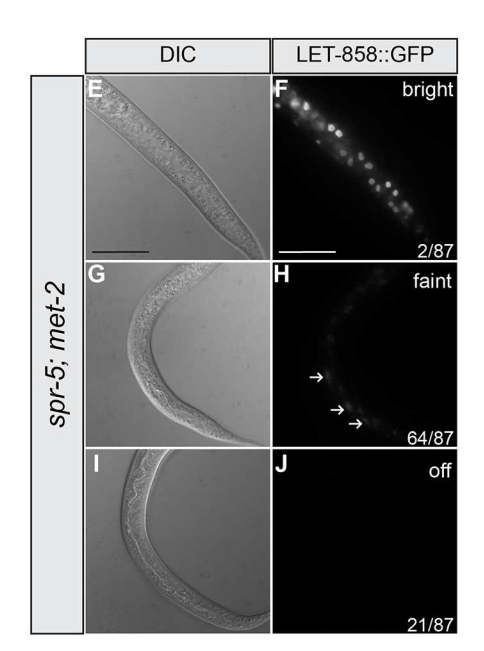


Fig. 7. let-858 transgene silencing in the soma of spr-5; met-2 mutants. (A-J) Representative 40× differential contrasting interference (DIC) (A,C,E,G,I) and immunofluorescent (B,D,F,H,J) images of wild-type (A-D) and spr-5; met-2 (E-J) L2 progeny. Arrows denote faint expression of LET-858::GFP. (K) Percentage of animals in which the expression level of LET-858::GFP was scored as either bright expressing (bright green, representatives shown in panels B and F), faint expressing (dark green, representatives shown in panels D and H) or not expressing (black, representative shown in panel J) in wild-type (N=132) versus spr-5; met-2 (N=87) progeny. The quantification represents the percentages of LET-858::GFP expressing progeny from two independent experiments. To control for the segregation of the let-858 transgene, progeny scored as 'off' were normalized for the presence of the let-858 transgene in animals as detected by PCR (see Materials and Methods). Scale bars: 50 µm.

less than 50% of progeny inherited the *let-858* transgene, we normalized the percentage of progeny scored as 'off' for LET-858:: GFP to the presence of the *let-858* transgene based on genotyping for *gfp* (see Materials and Methods). For wild type, all of the 60 L2 progeny that were scored as 'off' failed to inherit the *let-858* transgene, indicating that the transgene is never silenced in wild-type progeny. However, for *spr-5*; *met-2* L2 progeny, eight out of 50 progeny that were scored as 'off' inherited the *let-858* transgene, indicating that the *let-858* transgene can be completely silenced in some *spr-5*; *met-2* progeny. After normalization for the transgene inheritance, we observed that 21/87 of *spr-5*; *met-2* progeny displayed no visible expression of the *let-858::GFP* transgene (Fig. 7I,J,K).

### **DISCUSSION**

# spr-5; met-2 maternal reprogramming prevents developmental delay by restricting ectopic MES-4 bookmarking

SPR-5 and MET-2 act maternally to reprogram histone methylation and prevent the transcriptional state of the parent from being inappropriately transmitted to the offspring (Kerr et al., 2014). In this study, we found that the loss of SPR-5 and MET-2 maternal reprogramming led to a severe developmental delay that was associated with the ectopic expression of MES-4 germline genes in somatic tissues. This finding raises the possibility that SPR-5 and MET-2 reprogramming blocks the ectopic expression of MES-4

germline genes by preventing the accumulation of MES-4-dependent H3K36me3 at a subset of germline genes in somatic tissues. Consistent with this possibility, most of the MES-4 germline genes were increased in *spr-5; met-2* mutants compared with wild type in L1 larvae. Using smFISH, we confirmed the somatic expression of two ectopically expressed MES-4 germline genes, *htp-1* and *cpb-1*. Although *htp-1* mRNA was ectopically detected in many somatic tissues, the ectopic expression of *cpb-1* mRNA was more restricted, suggesting that the extent of ectopic expression is dependent upon the locus. However, further experiments are required to determine why some MES-4 germline genes may be more ectopically expressed than others.

In the absence of SPR-5 and MET-2 reprogramming, MES-4 germline genes accumulate ectopic H3K36me3 in the soma. This suggests that, without SPR-5 and MET-2 reprogramming, MES-4 ectopically maintains H3K36me3 at these genes in somatic tissues. Consistent with this finding, Greer et al. have previously reported that there are elevated bulk levels of H3K36me3 in mixed populations of *spr-5* single mutants (Greer et al., 2014). Of note, we observed a low level of H3K36me3 at germline genes in the somatic tissues of wild-type progeny. It is unclear why there is a low level of H3K36me3 normally in somatic tissues in wild-type animals. Nevertheless, the absence of transcription associated with this low level of H3K36me3 indicates that an increased level of H3K36me3 is necessary to cause ectopic transcription.

If the ectopic maintenance of H3K36me3 in the soma of *spr-5; met-2* mutant progeny is causing the developmental delay, then removal of MES-4 should rescue the ectopic expression and developmental delay. Indeed, we found that the removal of MES-4 rescued both the ectopic transcription of MES-4 germline genes in the soma of *spr-5; met-2* progeny, and the developmental delay. Taken together, our data provide evidence that the developmental delay of *spr-5; met-2* progeny is caused by the ectopic expression of MES-4 germline genes.

# How does an ectopic transcriptional program interfere with developmental timing?

How does the ectopic expression of germline genes interfere with somatic tissues to cause developmental delay? One possibility is that the ectopic expression of MES-4 germline genes causes the soma to take on germline characteristics. To begin to address this, we asked whether *spr-5; met-2* double mutants can silence an extrachromosomal array in somatic tissues. The silencing of extrachromosomal arrays is normally restricted to the germline (Kelly and Fire, 1998). However, we found that *spr-5; met-2* progeny acquired some ability to silence an extrachromosomal multicopy array in somatic cells. Consistent with this finding, loss of the somatic repressor LIN-35 also resulted in the somatic silencing of a GFP transgene (Wang et al., 2005), suggesting that LIN-35 also contributes to the repression of germline genes in somatic tissues.

In the *spr-5; met-2* mutant RNA-seq we detected the ectopic expression of RNA-dependent RNA polymerase genes (e.g. *rrf-1* and *gld-2*) as well as genes involved in the RNAi effector complex (e.g. *hrde-1* and *ppw-1*) (Table S13). These pathways have previously been implicated in gene silencing (Buckley et al., 2012; Sijen et al., 2001; Tijsterman et al., 2002). Thus, similar to what has been found in *lin-35* mutants (Wang et al., 2005), it is possible that the somatic silencing of the transgene in *spr-5; met-2* mutants is due to the induction of the germline small RNA pathway. In a reciprocal fashion, heritable silencing via small RNAs requires MET-2 (Lev et al., 2017). This interaction between MET-2 and small RNAs in the germline is consistent with the possibility that the chromatin and small RNA pathways may also be functioning together in the soma.

Normally in L1 larvae, the primordial germ cells, Z2 and Z3, are arrested at the G2/M checkpoint (Fukuyama et al., 2006). In the spr-5; met-2 mutant RNA-seq, we detected the ectopic expression of genes involved in the negative regulation of proliferation and the cell cycle, as well as G2/M checkpoint genes. Thus, it is possible that ectopic expression of germline genes normally expressed only in Z2 and Z3 contributes to the developmental delay through the ectopic activation of germline cell cycle control. Regardless, the silencing of the extrachromosomal multicopy array suggests that the somatic tissues in spr-5; met-2 progeny make functional proteins that can perform some germline functions. We propose that either ectopic germline transcription, or an ectopic germline function resulting from this ectopic transcription, interferes with the ability of somatic cells to properly enact their transcriptional program. This background noise delays the proper adoption of cell fate, leading to an overall delay in the development of the tissue.

# A model for how the inheritance of histone methylation is balanced to specify germline versus soma

By linking maternal *spr-5; met-2* reprogramming to the MES-4 germline inheritance system, our data provide a rationale for the existence of MES-4 bookmarking, through the following model. *spr-5; met-2* reprogramming prevents H3K4me2 transcriptional memory from being inappropriately propagated from one

generation to the next. MES-4 antagonizes this reprogramming to help germline genes reactivate in the embryonic germline. When *spr-5; met-2* reprogramming is defective, MES-4 ectopically maintains H3K36me3 in the soma, causing developmental delay.

The model that we are proposing is based on the following evidence. In the germline, transcriptional elongation is blocked by PIE-1, which segregates to germline blastomeres during embryogenesis (Batchelder et al., 1999; Mello et al., 1992; Seydoux et al., 1996) (Fig. 8A,B). In the soma of the early embryo, there is also very little transcription, because the bulk of zygotic transcription does not begin until approximately the 60-cell stage. This stage is just before when the primordial germ cells, Z2 and Z3, are specified (Sulston et al., 1983). Thus, in *C. elegans*, germline versus soma is largely specified without transcription.

During normal maternal reprogramming, SPR-5 and MET-2 are deposited into the oocyte. At fertilization they facilitate the reprogramming of previously expressed genes from an active chromatin state to a repressed chromatin state by removing H3K4me2 and adding H3K9me2 (Kerr et al., 2014) (Fig. 8A). This reprogramming is necessary to prevent the transcriptional memory of the previous generation from being inappropriately propagated to the progeny. Genes epigenetically reprogrammed by SPR-5 and MET-2 include ubiquitously expressed genes and germline-expressed genes, a subset of which are MES-4 germline genes. The MES-4 germline genes are subsequently targeted by the transcription-independent H3K36 methyltransferase, MES-4, to maintain H3K36me3 in the germ lineage during embryogenesis (Fig. 8A,B). We propose that H3K36 methylation bookmarking antagonizes the repression caused by the erasure of H3K4me2 and the addition of H3K9me2. Without the transcription-independent maintenance of inherited H3K36 methylation from the mother to antagonize this repression, the germline fails to proliferate and animals are sterile (Capowski et al., 1991; Garvin et al., 1998). The failure to proliferate and sterility caused by loss of MES-4 may be in part because germline genes that are targeted by MES-4 fail to reactivate, though it has yet to be demonstrated. Thus, the MES-4 bookmarking system may be necessary for crucial germline genes to bypass the global epigenetic reprogramming that occurs at fertilization to prevent transgenerational inheritance. We refer to this initial phase of filtering inherited histone methylation at fertilization as the establishment phase. Importantly, as multiple studies have shown that small RNAs are required for transgenerational inheritance (Ashe et al., 2012; Buckley et al., 2012; Lev et al., 2017), it is possible that small RNAs facilitate the inheritance of MES-4-dependent H3K36 methylation. The ectopic expression of some RNA machinery in *spr-5*; *met-2* double mutants hints at this potential connection. However, no direct link has been found yet between small RNAs and the MES-4 inheritance system.

Following this establishment phase, a maintenance phase is required to propagate this initial pattern of histone methylation throughout embryogenesis. The MES-4 bookmarking system is localized primarily to the primordial germ cells in later embryonic development (Furuhashi et al., 2010; Rechtsteiner et al., 2010). This concentration of MES-4 to the germline helps to maintain MES-4 bookmarking for germline specification later in embryonic development. However, MES-4 is also present in somatic cells (Furuhashi et al., 2010; Rechtsteiner et al., 2010). This makes germline genes targeted by MES-4 vulnerable to the ectopic maintenance of H3K36me3 bookmarking by MES-4 in the soma. Consistent with MES-4 being present in somatic cells during embryogenesis, we first detected the ectopic expression of *htp-1* in the embryo after zygotic genome activation. The presence of MES-4

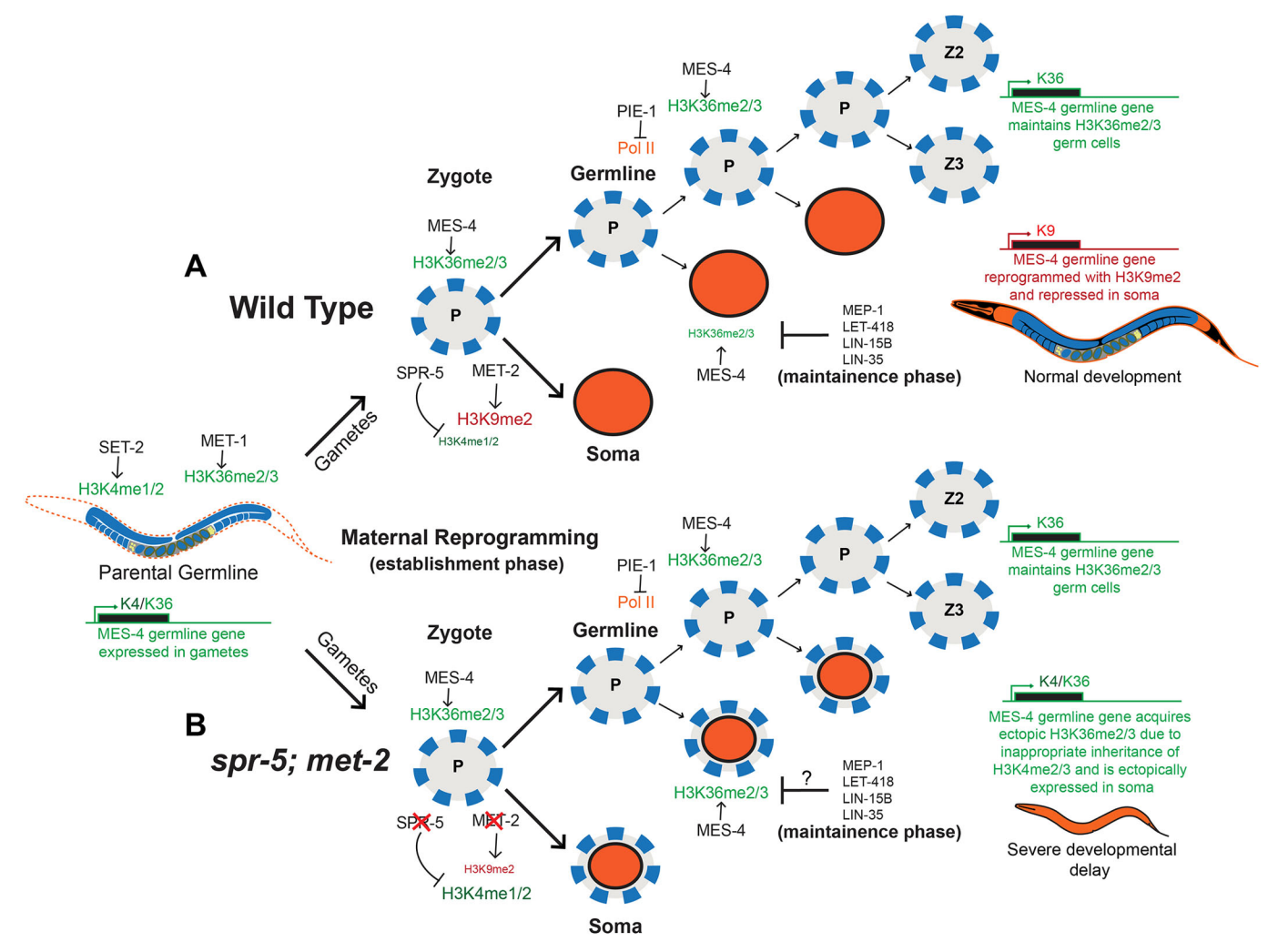


Fig. 8. A model for how maternal reprogramming of inherited histone methylation helps to specify germline versus soma. (A) During development, SET-2 and MET-1 add transcriptionally coupled H3K4me1/2 and H3K36me2/3 to germline-expressed genes in the parental germline, respectively. At fertilization, these germline-expressed genes undergo maternal epigenetic reprogramming (establishment phase) by SPR-5 and MET-2 to remove H3K4me1/2 and add H3K9me1/2. In the germline blastomeres of the embryo, PIE-1 prevents global transcription by inhibiting POL-II. In the absence of transcription, MES-4 maintains H3K36me2/3 at MES-4 germline genes that have acquired transcriptionally coupled H3K36me2/3 in the previous germline. This enables these genes to avoid being repressed by maternal *spr-5; met-2* reprogramming and ensures that these genes remain bookmarked for re-expression once the germline begins to proliferate later in development. In addition, multiple systems, such as LIN-15B and LIN-35, as well as MEP-1 and LET-418, function in somatic tissues to further antagonize H3K36 bookmarking by MES-4 (maintenance phase). (B) Without SPR-5 and MET-2 maternal reprogramming, H3K4me1/2 is inappropriately inherited in somatic tissues, allowing MES-4 to ectopically add H3K36me2/3 at these germline genes. This leads to ectopic expression of MES-4 germline genes in somatic tissues and a severe developmental delay. Orange circles represent somatic cells, gray circles outlined in blue dashed-lines represent germ cells and orange circles outlined in dashed-blue lines depict somatic cells that ectopically express MES-4 germline genes. P-lineage germline blastomeres are indicated by the letter P, and the primordial germline cells are indicated by Z2 and Z3.

in somatic cells during embryogenesis may explain why additional transcriptional repressors, such as LIN-15B and LIN-35, as well as MEP-1 and LET-418, function in somatic tissues to restrict H3K36 bookmarking by MES-4 to the germline. Thus, in the maintenance phase, the balance of MES-4 and the pathways that somatically antagonize MES-4 maintain the histone methylation pattern that is initiated during the establishment phase. Interestingly, LET-418 may also help to maintain SPR-5 repression in the *C. elegans* germline, as SPR-5 and LET-418 have been shown to function synergistically to prevent somatic reprogramming of germline stem cells (Käser-Pébernard et al., 2014). Taken together, we propose that SPR-5, MET-2 and MES-4 carefully balance the inheritance of three different histone modifications, H3K4, H3K9 and H3K36 methylation, to ensure the proper specification of germline versus soma in the absence of transcription.

The model that we have proposed makes the following two predictions. First, MES-4 germline genes should normally be targeted for continued silencing by H3K9me2 in somatic tissues. It has recently been shown that a subset of germline-specific genes contain H3K9me2 at their promoters in somatic tissues (Rechtsteiner et al., 2019). We re-examined the H3K9me2 ChIP-seq dataset from this work and found that the MES-4 germline genes that are ectopically expressed in the somatic tissues of *spr-5; met-2* progeny also displayed unique H3K9me2 promoter peaks. This confirms that MES-4 germline genes are normally repressed by H3K9me2 in somatic tissues.

The second prediction from our model is that the ectopic inheritance of H3K4 methylation at MES-4 germline genes overwhelms the somatic repression systems. Despite the presence of these transcriptional repressor complexes and chromatin

remodelers to antagonize MES-4 bookmarking in the soma, loss of spr-5; met-2 maternal reprogramming results in the somatic expression of MES-4 germline genes. This suggests that the failure to add H3K9me2, as well as the inappropriate retention of H3K4me2, results in a chromatin environment that is permissive for the ectopic maintenance of H3K36me3 in the soma, even in the presence of the pathways that repress MES-4 bookmarking somatically (Fig. 8B). If this is the case, then the developmental delay in spr-5; met-2 progeny should also be dependent upon the activity of the H3K4 methyltransferase. We found that RNAimediated depletion of SET-2, the H3K4me1/2 methyltransferase, rescued the developmental delay that we observed in spr-5; met-2 progeny. These findings suggest that the inheritance of ectopic H3K4 methylation enables the ectopic accumulation of MES-4dependent H3K36me3, and the subsequent ectopic expression of MES-4 germline genes in somatic tissues of *spr-5*: *met-2* progeny. Consistent with SPR-5 and MET-2 functioning directly at MES-4 targets, we found no evidence of ectopic MES-4 in spr-5; met-2 progeny. It is not entirely clear how the subsequent ectopic maintenance of H3K36me3 facilitates ectopic expression. However, it should be noted that there were some differences in which MES-4 germline genes were ectopically expressed between our two spr-5; met-2 RNA-seq experiments. This stochasticity is consistent with H3K36me3 being permissive, rather than instructive, for transcription. If this is the case, it is doubtful that the spr-5; met-2 developmental delay is caused by the inappropriate expression of any single MES-4 germline gene. Rather, it is likely that the developmental delay is caused by either the inappropriate expression of multiple MES-4 germline genes, or the ectopic activation of the MES-4 germline program.

The model that we have presented here is composed of two phases, an initiation phase and a maintenance phase. The timing of these two phases is consistent with the known expression patterns of the enzymes in *C. elegans*. For example, maternal SPR-5 is present in the early embryo up to the eight-cell stage, but gone in later embryos (Katz et al., 2009). In contrast, maternal MES-4 continues to be expressed in much later-staged embryos (Rechtsteiner et al., 2010). The timing presented in our model is also partially based on the known requirement for maternal LSD1 (vertebrate SPR-5 ortholog) to function between fertilization and the two-cell stage in mice (Wasson et al., 2016). Nevertheless, no definitive evidence exists that the two phases are distinct timing wise. Thus, further investigation will be required to substantiate the proposed timing in our model.

# Conservation of maternal epigenetic reprogramming between invertebrates and vertebrates

Epigenetic reprogramming at fertilization is a problem that all sexually reproducing organisms must solve (Lee and Katz, 2020). Thus, it is possible that the mechanisms of epigenetic reprogramming may be conserved. Along with the Heard lab, we have previously demonstrated that progeny from mice that lack maternal LSD1 ectopically maintain the expression of germline genes in the embryo, leading to embryonic arrest at the two-cell stage (Ancelin et al., 2016; Wasson et al., 2016). Similarly, maternal loss of the MET-2 ortholog SETDB1 or the MES-4 ortholog NSD1 in mice results in early embryonic lethality (Kim et al., 2016; Rayasam et al., 2003). Together, these results underscore the developmental importance of properly regulating histone methylation between generations and raise the possibility that the mechanism we have uncovered is conserved in mammals.

The model that we have proposed may also help explain the mechanism underlying patients harboring mutations in various histone-modifying enzymes. Recent genome sequencing has revealed that several neurodevelopmental disorders are caused by mutations in histone-modifying enzymes (extensively reviewed by Kim et al., 2017). These include mutations in: (1) the H3K36 methyltransferase SETD2 and the H3K27 demethylase KDM6A, which cause Kabuki Syndrome (Lederer et al., 2012); (2) the human ortholog of spr-5, LSD1, which causes a Kabuki-like Syndrome (Chong et al., 2016; Tunovic et al., 2014); (3) the H3K36 methyltransferase NSD1 which causes Sotos Syndrome (Kurotaki et al., 2002). Similar to what we observed in spr-5; met-2 mutant progeny, many of the human patients with mutations in these histone modifying enzymes suffer from global developmental delay. Based on our model, it is possible that the developmental delay in these patients may be caused by the failure to properly regulate histone methylation during crucial developmental transitions. The resulting inappropriate inheritance of histone methylation could result in the ectopic expression of a developmental program in an inappropriate tissue, leading to background noise and developmental delay.

# MATERIALS AND METHODS

#### **Strains**

All C. elegans strains were grown and maintained at 20°C under standard conditions, as previously described (Brenner, 1974). The C. elegans spr-5 (by101)(I) strain was provided by R. Baumeister (Albert Ludwig University of Freiburg, Germany). The N2 Bristol wild-type (wild type) strain was provided by the Caenorhabditis Genetics Center. The met-2 (n4256)(III) strain was provided by R. Horvitz (Massachusetts Institute of Technology, MA, USA). The mes-4(bn149(mes-4::gfp::ha::6xhis))(V) strain was provided by Susan Strome (The University of California, Santa Cruz, CA, USA). The hT2 [bli-4(e937)let-?(q782)qls48] (I;III) balancer strain was used to maintain spr-5 (by101)(I); met-2 (n4256)(III) double-mutant animals as heterozygotes. Because the hT2 [bli-4(e937)let-?(q782)qls48](I;III) balancer allele does not extend completely to the spr-5 locus on chromosome I, the F0 animals used to generate F1 spr-5; met-2 progeny were cloned out and genotyped to confirm the presence of the spr-5 (by101)(I) allele. For genotyping, single animals were picked into 5-10 µl of lysis buffer [50 mM KCl, 10 mM Tris-HCl (pH 8.3), 2.5 mM MgCl<sub>2</sub>, 0.45% NP-40, 0.45% Tween-20, 0.01% gelatin] and incubated at 65°C for 1 h followed by 95°C for 30 min. PCR reactions were performed with AmpliTaq Gold (Invitrogen) according to the manufacturer's protocol and reactions were resolved on agarose gels (see Table S9 for genotyping primer sequences). Before completing this study we acquired the FX30208 tmC27 [unc-75(tmls1239)](I) from the Caenorhabditis Genetics Center that completely covers the spr-5 locus on chromosome I. The qC1 [qls26 (lag2::GFP+rol-6(su1006)](III) strain was obtained from W. Kelly (Emory University, GA, USA) and crossed to met-2 (n4256)(III) to maintain met-2(n4256)(III) as heterozygotes. The spr-5 (by101)(I)/tmC27[uncmet-2(n4256)(III)/qC1 [qls26 75(tmls1239)](I); (lag2::gfp+ 6(su1006))](III) strain was then re-created for this study to maintain spr-5 (by101)(I); met-2 (n4256)(III) double-mutant animals as balanced heterozygotes. The LET-858::GFP [pha-1(e2123ts)(III); let-858::gfp (ccEx7271)] (Kelly and Fire, 1998) transgenic strain used in somatic transgene silencing assays was acquired from W. Kelly.

### Scoring developmental delay

*C. elegans* adult hermaphrodites were allowed to lay embryos for 2-4 h and then removed in order to synchronize the development of progeny. Progeny were then imaged and scored for development to the adult stage at either 72 h or seven days after synchronized lay, depending on the experiment. To monitor embryogenesis, *C. elegans* adult hermaphrodites were dissected and the four-cell stage was established as the starting point, 0 min, for each strain. Subsequently, time-lapse images were obtained at 30 min, 60 min and 120 min.

# **RNA-seq and analysis**

Total RNA was isolated using TRIzol reagent (Invitrogen) from 200-250 starved L1 larvae born at room temperature (21°C-22°C) overnight in M9

Buffer. Owing to the difficulty in isolating large numbers of spr-5; met-2 double-mutant progeny from the hT2 [bli-4(e937)let-?(q782)qls48](I;III) balancer strain, we submitted total RNA to the Genomic Services Laboratory, HudsonAlpha Institute for Biotechnology (GSL) for low input RNA-seq services. This service uses the Ovation RNA-Seq System V2 kit (Nugen) for initial RNA amplification before library preparation and sequencing (Illumina HiSeq v4, 50 bp paired-end reads). For each genotype, two biological replicates were obtained. During the course of these experiments, the FX30208 tmC27 [unc-75(tmls1239)](I) balancer became available from the Caenorhabditis Genetics Center. This balancer completely covers the spr-5 locus on chromosome I. Using this balanced strain, we performed a repeat spr-5; met-2 RNA-seq experiment with three additional biological replicates of spr-5; met-2 versus wild-type L1 progeny. We submitted the total RNA from new replicates of the repeat RNA-seq to Georgia Genomics and Bioinformatics Core (University of Georgia, GA, USA) for standard Poly-A RNA-seq services (Illumina Nextseq, 50 bp paired-end reads). Downstream quality control and analysis were performed identically for both RNA-seq experiments. For both the low-input and repeat standard RNA-seq, sequencing reads were checked for quality using FastQC (Wingett and Andrews, 2018), filtered using Trimmomatic (Bolger et al., 2014) and remapped to the *C. elegans* transcriptome (ce10, WS220) using HISAT2 (Kim et al., 2015). Read count by gene was obtained by FeatureCounts (Liao et al., 2014). Differentially expressed transcripts for the low-input RNA-seq experiment (significance threshold, Wald test, P-value <0.05) and the repeat RNA-seq experiment (significance threshold, Wald test, P-adj<0.05) were determined using DESEQ2 (v.2.11.40.2) (Love et al., 2014). Transcripts per million (TPM) values were calculated from raw data obtained from FeatureCounts output. Subsequent downstream analysis was performed using R with normalized counts and P-values from DESEQ2 (v.2.11.40.2). Heatmaps were produced using the ComplexHeatmap R Package (Gu et al., 2016). Data were scaled and hierarchical clustering was performed using the complete linkage algorithm. In the linkage algorithm, distance was measured by calculating pairwise distance. Volcano plots were produced using the EnhancedVolcano package (v.0.99.16). In addition, GO Pathway analysis was performed using the online platform WormEnrichr (Chen et al., 2013; Kuleshov et al., 2016). R scripts for heatmaps, volcano plots and GO analysis have been deposited into GEO under accession code GSE143839. Rechtsteiner and colleagues identified 214 MES-4 germline genes (Rechtsteiner et al., 2010): 17 of these genes are pseudogenes that we were unable to convert from Ensembl transcript IDs to RefSeq mRNA accession, and another gene was duplicated, so we removed those genes. This leaves 196 MES-4 germline genes that we used for our analysis. An additional heatmap comparison of differentially expressed genes between spr-5, met-2 and spr-5; met-2 progeny compared with wildtype progeny was generated in Microsoft Excel using log2 fold change values from the DESEQ2 analysis. Because transcript isoforms were ignored, we discuss the data in terms of 'genes expressed' rather than 'transcripts expressed'.

### **ChIP-seq and analysis**

ChIP experiments were performed as described by Katz et al. (2009). Briefly, 600 starved L1 larvae born at room temperature (21°C-22°C) overnight in M9 Buffer were collected, frozen in liquid nitrogen and stored at -80°C before homogenization. Frozen pellets were disrupted by a glass Dounce homogenizer, fixed with formaldehyde (1% final concentration) and quenched with glycine. ChIP samples were processed with a Chromatin Immunoprecipitation Assay Kit (Millipore), according manufacturer's instructions. Samples were sonicated using a Diagenode Bioruptor UCD-200 at 4°C on the 'high' setting for a total of 30 min with a cycle of 45 s on and 15 s off. A total of 12.5 μL (5 μg) H3K36me3 antibody (61,021; Active Motif) was used for immunoprecipitation. The GSL performed library preparation and sequencing (Illumina HiSeq v4, 50 bp single-end reads). Reads were checked for quality using FastQC (Wingett and Andrews, 2018) and remapped to the C. elegans transcriptome (ce10, WS220) using Bowtie2 (Langmead and Salzberg, 2012; Langmead et al., 2009) under default parameters. bamCoverage in deepTools2 (Ramírez et al., 2016) was used to generate bigwig coverage tracks in 50 bp bins, with blacklisted regions from McMurchy et al. (2017) excluded, using the

following parameters: -bs 50, -normalizeUsing RPKM (McMurchy et al., 2017). MACS2 (Feng et al., 2012; Zhang et al., 2008) default parameters were used to call peaks and create bedgraph files for sequenced and mapped H3K36me3 ChIP samples and input DNA samples with the following adjustments to account for H3K36me3 broader domains: Broad-cutoff = 0.001. Blacklisted regions from McMurchy et al. (2017) were excluded for this analysis. Using published H3K36me3 modMine Chip-chip called broad peaks (modENCODE\_3555) from wild-type L1 larvae as a guide, we then merged called broad peaks within 1200 bp using Bedtools: MergeBED (Quinlan and Hall, 2010). H3K9me2 bedgraph files used in our analysis were from a published dataset (Rechtsteiner et al., 2019). Integrative Genome Viewer (IGV) was used to visualize H3K36me3 reads normalized to reads per kilobase millions (RPKM) and H3K9me2 reads normalized to 15 million reads (genome-wide coverage of H3K9me2; Rechtsteiner et al., 2019).

#### **RNAi** methods

RNAi by feeding was carried out using clones from the Ahringer library (Kamath and Ahringer, 2003). Feeding experiments were performed on RNAi plates (NGM plates containing 100 µg/ml ampicillin, 0.4 mM IPTG, and 12.5 µg/ml tetracycline). F0 worms were placed on RNAi plates as L2 larvae and then moved to fresh RNAi plates 48 h later where they were allowed to lay embryos for 2-4 h. F0 worms were then removed from plates and sacrificed or placed in M9 buffer overnight so that starved L1 progeny could be isolated for quantitative PCR (qPCR). F1 progeny were scored 72 h after the synchronized lay for developmental progression. For each RNAi experiment, *pos-1* RNAi was used as a positive control. For each RNAi experiment reported here, *pos-1* RNAi resulted in >95% embryonic lethality, indicating that RNAi plates were optimal.

### **Real-time expression analysis**

Total RNA was isolated using TRIzol reagent (Invitrogen) from synchronized L1s born at room temperature (21°C-22°C). cDNA synthesis and qPCR were carried out as previously described (Kerr et al., 2014). A total of two biological replicates were performed and for both biological replicates experiments were performed in triplicate and normalized to *ama-1* mRNA expression (see Table S10 for RT-PCR primer sequences).

### **Differential interference contrast microscopy**

Worms were immobilized in 0.1% levamisole and placed on a 2% agarose pad for imaging at either  $10\times$  or  $40\times$  magnification. The  $40\times$  DIC images were overlaid together using Adobe Photoshop to generate high resolution images of whole worms. For the embryogenesis time course, dissected four-cell embryos were mounted on a 2% agarose pad, covered with a coverslip and sealed with petroleum jelly. Embryos were imaged at  $100\times$  magnification.

## smFISH

Quasar 570-labeled smFISH probe sets for htp-1 and cpb-1 were designed using Stellaris Probe Designer (Biosearch) (see Tables S7,S8 for probe sequences). The htp-1 smFISH probes were designed using the complete 1059nt htp-1 protein-coding sequence. Likewise, the cpb-1 smFISH probes were designed using the complete 1683nt *cpb-1* protein-coding sequence. In addition, an smFISH fluorescent probe set for ama-1 was purchased from the DesignReady catalog (VSMF-6002-5, Biosearch). Synchronized L1 larvae for smFISH were obtained by bleaching 300-500 hermaphrodites and allowing embryos to hatch overnight on 6 cm NGM plates lightly seeded with OP50 bacteria. L1 larvae were then washed into 1.5 µl Eppendorf tubes using nuclease-free M9 buffer. Fixation and hybridization steps followed the Stellaris RNA FISH protocol for C. elegans adapted from the Raj lab protocol (Raj and Tyagi, 2010). In brief, we resuspended L1 larvae in fixation buffer (3.7% formaldehyde in 1×PBS) for 15 min at room temperature then transferred tubes to liquid nitrogen. Samples were thawed in water and placed on ice for 20 min. We obtained better fluorescent signal by freeze cracking L1 larvae. Following fixation, L1 larvae were resuspended in 70% EtOH and stored at 4°C for 24-48 h. For all probe sets, we incubated L1 larvae in 100 µl hybridization buffer

(containing 10% formamide and 125 nm probe) for 4 h at 37°C. After hybridization, samples were washed in wash buffer at 37°C for 30 min, incubated in 50 ng/mL DAPI in wash buffer at 30°C for 30 min, washed once in 2× SSC for 2 min at room temperature and mounted in Vectashield mounting medium. Mounted slides were imaged immediately using a 100× objective on a spinning-disk confocal Nikon-TiE imaging system. Images were captured using NIS-Elements software (Nikon), and ImageJ (http://imagej.nih.gov/ij/) was used for viewing. ImageJ maximum projection was used to project z-stack images to a single plane. The fluorescent intensity of smFISH dots were >2-fold above background as expected (Ji and van Oudenaarden, 2012).

## Immunofluorescence staining

L1 larvae were permeabilized on slides using the freeze-crack method and immediately fixed with methanol/acetone as previously described (Duerr, 2013). Following fixation, slides were washed once with 1× PBST (phosphate buffer saline with 0.1% Tween-20) then blocked for 30 min in Antibody Buffer (1× PBST with 0.5% bovine serum albumin and 0.01% sodium azide). Primary antibody staining to detect the mes-4(bn149(mes-4:: gfp::ha::6xhis))(V) allele was performed overnight at room temperature using a rabbit polyclonal anti-GFP antibody (ab6556, Abcam) at a 1:500 dilution. After three washes with 1× PBST, secondary antibody staining was performed for 1 h at room temperature using an Alexa Fluor 594-conjugated goat anti-rabbit antibody (A32740, Invitrogen) at a 1:500 dilution. Following incubation with secondary antibody, slides were washed twice with 1× PBST and once with 1× PBST containing 200 ng/ml DAPI. After three washes with 1× PBST, slides were mounted in Vectashield mounting medium and imaged immediately using a  $100\times$  objective on a spinning-disk confocal Nikon-TiE imaging system.

### LET-858::GFP transgene silencing assay

First generation spr-5; met-2 hermaphrodites were crossed to let-858 transgenic males to generate spr-5/+; met-2/+; let-858::gfp animals. The let-858 transgene is an extrachromosomal multicopy let-858 array (Kelly and Fire, 1998). From these animals we generated spr-5; met-2; let-858::gfp animals and scored them for somatic expression of LET-858::GFP using a standard stereoscope. L2 progeny from wild-type and spr-5; met-2 progeny expressing the let-858::GFP transgene were scored as 'bright' (high level ubiquitous expression), 'faint' (barely visible and ubiquitous expression) or 'off' (no expression). Because <50% of progeny inherited the let-858 transgene, we normalized the percentage of progeny scored as 'off' for LET-858::GFP to the presence of the let-858 transgene based on genotyping for gfp. For wild type, 0 out of 60 progeny that were scored as 'off' failed to inherit the let-858 transgene, indicating that the transgene is never silenced in wild-type progeny (see Table S9 for gfp genotyping primer sequences). For spr-5; met-2 progeny, 8 out of 50 progeny that were scored as 'off' inherited the let-858 transgene, indicating that the let-858 transgene is completely silenced in some *spr-5*; *met-2* progeny.

### Acknowledgements

We are grateful to members of the Katz lab, as well as T. Caspary and C. Bean, for their helpful discussion and critical reading of the manuscript; M. J. Rowley for advice on bioinformatics; S. Strome and L. Petrella for helpful discussion and experimental advice; C. Cockrum in the Strome lab for sharing the transgenic MES-4 strain in advance of publication; D. Lerit, R. Deal, V. Corces and W. Kelly for the generous sharing of reagents and equipment. We thank R. Horvitz, W. Kelly and the *Caenorhabditis* Genetics Center (funded by NIH P40 OD010440) for strains.

## Competing interests

The authors declare no competing or financial interests.

## Author contributions

Conceptualization: B.S.C., T.W.L., D.J.K.; Methodology: B.S.C., T.W.L., D.J.K.; Software: D.A.M.; Validation: B.S.C., D.J.K.; Formal analysis: B.S.C., C.F.P., J.S.B., D.A.M., D.J.K.; Investigation: B.S.C., C.F.P., J.D.R., J.S.B., D.J.K.; Resources: B.S.C., D.J.K.; Data curation: B.S.C., D.A.M., D.J.K.; Writing - original draft: B.S.C.; Writing - review & editing: B.S.C., T.W.L., D.J.K.; Visualization: B.S.C., D.J.K.; Supervision: B.S.C., D.J.K.; Project administration: B.S.C., D.J.K.; Funding acquisition: B.S.C., D.J.K.

#### **Funding**

This work was funded by a Division of Integrative Organismal Systems grant to D.J.K. (NSF IOS1931697); T.W.L. and B.S.C. were supported by National Institutes of Health Fellowships in Research and Science Teaching IRACDA postdoctoral program (NIH K12GM00680-15); B.S.C. and J.D.R. were supported by the National Institutes of Health (NIH F32 GM126734-01 and NIH F31 HD100145, respectively). Deposited in PMC for release after 12 months.

#### Data availability

Raw and processed genomic data has been deposited in GEO under accession number GSE143839.

#### Supplementary information

Supplementary information available online at https://dev.biologists.org/lookup/doi/10.1242/dev.196600.supplemental

#### Peer review history

The peer review history is available online at https://dev.biologists.org/lookup/doi/10.1242/dev.196600.reviewer-comments.pdf

#### References

- Alvares, S. M., Mayberry, G. A., Joyner, E. Y., Lakowski, B. and Ahmed, S. (2014). H3K4 demethylase activities repress proliferative and postmitotic aging. *Aging Cell* 13, 245-253. doi:10.1111/acel.12166
- Ancelin, K., Syx, L., Borensztein, M., Ranisavljevic, N., Vassilev, I., Briseño-Roa, L., Liu, T., Metzger, E., Servant, N., Barillot, E. et al. (2016). Maternal LSD1/KDM1A is an essential regulator of chromatin and transcription landscapes during zygotic genome activation. *Elife* 5, 4615. doi:10.7554/eLife.08851
- Ashe, A., Sapetschnig, A., Weick, E.-M., Mitchell, J., Bagijn, M. P., Cording, A. C., Doebley, A.-L., Goldstein, L. D., Lehrbach, N. J., Le Pen, J. et al. (2012). piRNAs can trigger a multigenerational epigenetic memory in the germline of C. elegans. *Cell* 150, 88-99. doi:10.1016/j.cell.2012.06.018
- Bannister, A. J., Schneider, R., Myers, F. A., Thorne, A. W., Crane-Robinson, C. and Kouzarides, T. (2005). Spatial distribution of di- and tri-methyl lysine 36 of histone H3 at active genes. J. Biol. Chem. 280, 17732-17736. doi:10.1074/jbc. M500796200
- Barski, A., Cuddapah, S., Cui, K., Roh, T.-Y., Schones, D. E., Wang, Z., Wei, G., Chepelev, I. and Zhao, K. (2007). High-resolution profiling of histone methylations in the human genome. *Cell* 129, 823-837. doi:10.1016/j.cell.2007. 05.009
- Batchelder, C., Dunn, M. A., Choy, B., Suh, Y., Cassie, C., Shim, E. Y., Shin, T. H., Mello, C., Seydoux, G. and Blackwell, T. K. (1999). Transcriptional repression by the Caenorhabditis elegans germ-line protein PIE-1. *Genes Dev.* 13, 202-212. doi:10.1101/gad.13.2.202
- Bernstein, B. E., Humphrey, E. L., Erlich, R. L., Schneider, R., Bouman, P., Liu, J. S., Kouzarides, T. and Schreiber, S. L. (2002). Methylation of histone H3 Lys 4 in coding regions of active genes. *Proc. Natl. Acad. Sci. USA* **99**, 8695-8700. doi:10.1073/pnas.082249499
- Bernstein, B. E., Kamal, M., Lindblad-Toh, K., Bekiranov, S., Bailey, D. K., Huebert, D. J., McMahon, S., Karlsson, E. K., Kulbokas, E. J., Gingeras, T. R. et al. (2005). Genomic maps and comparative analysis of histone modifications in human and mouse. *Cell* 120, 169-181. doi:10.1016/j.cell.2005.01.001
- Bolger, A. M., Lohse, M. and Usadel, B. (2014). Trimmomatic: a flexible trimmer for Illumina sequence data. *Bioinformatics* **30**, 2114-2120. doi:10.1093/bioinformatics/btu170
- Brenner, S. (1974). The genetics of Caenorhabditis elegans. *Genetics* 77, 71-94. doi:10.1093/genetics/77.1.71
- Buckley, B. A., Burkhart, K. B., Gu, S. G., Spracklin, G., Kershner, A., Fritz, H., Kimble, J., Fire, A. and Kennedy, S. (2012). A nuclear Argonaute promotes multigenerational epigenetic inheritance and germline immortality. *Nature* 489, 447-451. doi:10.1038/nature11352
- Burton, A. and Torres-Padilla, M.-E. (2014). Chromatin dynamics in the regulation of cell fate allocation during early embryogenesis. *Nat. Rev. Mol. Cell Biol.* 15, 723-734. doi:10.1038/nrm3885
- Capowski, E. E., Martin, P., Garvin, C. and Strome, S. (1991). Identification of grandchildless loci whose products are required for normal germ-line development in the nematode Caenorhabditis elegans. *Genetics* 129, 1061-1072. doi:10.1093/genetics/129.4.1061
- Chen, E. Y., Tan, C. M., Kou, Y., Duan, Q., Wang, Z., Meirelles, G. V., Clark, N. R. and Ma'ayan, A. (2013). Enrichr: interactive and collaborative HTML5 gene list enrichment analysis tool. *BMC Bioinformatics* 14, 128. doi:10.1186/1471-2105-14-128
- Chong, J. X., Yu, J.-H., Lorentzen, P., Park, K. M., Jamal, S. M., Tabor, H. K., Rauch, A., Saenz, M. S., Boltshauser, E., Patterson, K. E. et al. (2016). Gene discovery for Mendelian conditions via social networking: de novo variants in KDM1A cause developmental delay and distinctive facial features. *Genet. Med.* 18, 788-795. doi:10.1038/gim.2015.161

- Duerr, J. S. (2013). Antibody staining in C. elegans using "freeze-cracking". J Vis Exp 80, 50664, doi:10.3791/50664
- Feng, J., Liu, T., Qin, B., Zhang, Y. and Liu, X. S. (2012). Identifying ChIP-seq enrichment using MACS. Nat. Protoc. 7, 1728-1740. doi:10.1038/nprot.2012.101
- Frum, T. and Ralston, A. (2015). Cell signaling and transcription factors regulating cell fate during formation of the mouse blastocyst. *Trends Genet.* **31**, 402-410. doi:10.1016/j.tig.2015.04.002
- Fukuyama, M., Rougvie, A. E. and Rothman, J. H. (2006). C. elegans DAF-18/ PTEN mediates nutrient-dependent arrest of cell cycle and growth in the germline. *Curr. Biol.* **16**, 773-779. doi:10.1016/j.cub.2006.02.073
- Furuhashi, H., Takasaki, T., Rechtsteiner, A., Li, T., Kimura, H., Checchi, P. M., Strome, S. and Kelly, W. G. (2010). Trans-generational epigenetic regulation of C. elegans primordial germ cells. *Epigenetics Chromatin* 3, 15. doi:10.1186/1756-8935-3-15
- Garvin, C., Holdeman, R. and Strome, S. (1998). The phenotype of mes-2, mes-3, mes-4 and mes-6, maternal-effect genes required for survival of the germline in Caenorhabditis elegans, is sensitive to chromosome dosage. *Genetics* 148, 167-185.
- Gaydos, L. J., Wang, W. and Strome, S. (2014). Gene repression. H3K27me and PRC2 transmit a memory of repression across generations and during development. Science 345, 1515-1518. doi:10.1126/science.1255023
- Greer, E. L., Beese-Sims, S. E., Brookes, E., Spadafora, R., Zhu, Y., Rothbart, S. B., Aristizábal-Corrales, D., Chen, S., Badeaux, A. I., Jin, Q. et al. (2014). A histone methylation network regulates transgenerational epigenetic memory in C. elegans. *Cell Rep.* 7, 113-126. doi:10.1016/j.celrep.2014.02.044
- Greer, E. L., Becker, B., Latza, C., Antebi, A. and Shi, Y. (2016). Mutation of C. elegans demethylase spr-5 extends transgenerational longevity. *Cell Res.* 26, 229-238. doi:10.1038/cr.2015.148
- Gregor, T., Garcia, H. G. and Little, S. C. (2014). The embryo as a laboratory: quantifying transcription in Drosophila. *Trends Genet.* 30, 364-375. doi:10.1016/j. tig.2014.06.002
- Gu, Z., Eils, R. and Schlesner, M. (2016). Complex heatmaps reveal patterns and correlations in multidimensional genomic data. *Bioinformatics* 32, 2847-2849. doi:10.1093/bioinformatics/btw313
- Hirabayashi, Y. and Gotoh, Y. (2010). Epigenetic control of neural precursor cell fate during development. *Nat. Rev. Neurosci.* 11, 377-388. doi:10.1038/nrn2810
- Jambhekar, A., Dhall, A. and Shi, Y. (2019). Roles and regulation of histone methylation in animal development. *Nat. Rev. Mol. Cell Biol.* 20, 625-641. doi:10. 1038/s41580-019-0151-1
- Ji, N. and van Oudenaarden, A. (2012). Single molecule fluorescent in situ hybridization (smFISH) of C. elegans worms and embryos. WormBook 1-16. doi:10.1895/wormbook.1.153.1
- Kamath, R. S. and Ahringer, J. (2003). Genome-wide RNAi screening in Caenorhabditis elegans. *Methods* 30, 313-321. doi:10.1016/s1046-2023(03)00050-1
- Kaneshiro, K. R., Rechtsteiner, A. and Strome, S. (2019). Sperm-inherited H3K27me3 impacts offspring transcription and development in C. elegans. *Nat. Commun.* **10**, 1271. doi:10.1038/s41467-019-09141-w
- Käser-Pébernard, S., Müller, F. and Wicky, C. (2014). LET-418/Mi2 and SPR-5/ LSD1 cooperatively prevent somatic reprogramming of C. elegans germline stem cells. Stem Cell Reports 2, 547-559. doi:10.1016/j.stemcr.2014.02.007
- Katz, D. J., Edwards, T. M., Reinke, V. and Kelly, W. G. (2009). A C. elegans LSD1 demethylase contributes to germline immortality by reprogramming epigenetic memory. Cell 137, 308-320. doi:10.1016/j.cell.2009.02.015
- Kelly, W. G. and Fire, A. (1998). Chromatin silencing and the maintenance of a functional germline in Caenorhabditis elegans. *Development* 125, 2451-2456.
- Kerr, S. C., Ruppersburg, C. C., Francis, J. W. and Katz, D. J. (2014). SPR-5 and MET-2 function cooperatively to reestablish an epigenetic ground state during passage through the germ line. *Proc. Natl. Acad. Sci. USA* 111, 9509-9514. doi:10.1073/pnas.1321843111
- Kim, D., Langmead, B. and Salzberg, S. L. (2015). HISAT: a fast spliced aligner with low memory requirements. *Nat. Methods* 12, 357-360. doi:10.1038/nmeth. 3317
- Kim, J., Zhao, H., Dan, J., Kim, S., Hardikar, S., Hollowell, D., Lin, K., Lu, Y., Takata, Y., Shen, J. et al. (2016). Maternal Setdb1 is required for meiotic progression and preimplantation development in mouse. *PLoS Genet.* 12, e1005970. doi:10.1371/journal.pgen.1005970
- Kim, J.-H., Lee, J. H., Lee, I.-S., Lee, S. B. and Cho, K. S. (2017). Histone lysine methylation and neurodevelopmental disorders. *Int. J. Mol. Sci.* 18, 1404. doi:10. 3390/ijms18071404
- Kreher, J., Takasaki, T., Cockrum, C., Sidoli, S., Garcia, B. A., Jensen, O. N. and Strome, S. (2018). Distinct roles of two histone methyltransferases in transmitting H3K36me3-based epigenetic memory across generations in caenorhabditis elegans. *Genetics* 210, 969-982. doi:10.1534/genetics.118.301353
- Kuleshov, M. V., Jones, M. R., Rouillard, A. D., Fernandez, N. F., Duan, Q., Wang, Z., Koplev, S., Jenkins, S. L., Jagodnik, K. M., Lachmann, A. et al. (2016). Enrichr: a comprehensive gene set enrichment analysis web server 2016 update. *Nucleic Acids Res.* 44, W90-W97. doi:10.1093/nar/gkw377
- Kurotaki, N., Imaizumi, K., Harada, N., Masuno, M., Kondoh, T., Nagai, T., Ohashi, H., Naritomi, K., Tsukahara, M., Makita, Y. et al. (2002).

- Haploinsufficiency of NSD1 causes Sotos syndrome. *Nat. Genet.* **30**, 365-366. doi:10.1038/ng863
- Langmead, B. and Salzberg, S. L. (2012). Fast gapped-read alignment with Bowtie 2. *Nat. Methods* **9**, 357-359. doi:10.1038/nmeth.1923
- Langmead, B., Trapnell, C., Pop, M. and Salzberg, S. L. (2009). Ultrafast and memory-efficient alignment of short DNA sequences to the human genome. *Genome Biol.* 10, R25. doi:10.1186/gb-2009-10-3-r25
- Lederer, D., Grisart, B., Digilio, M. C., Benoit, V., Crespin, M., Ghariani, S. C., Maystadt, I., Dallapiccola, B. and Verellen-Dumoulin, C. (2012). Deletion of KDM6A, a histone demethylase interacting with MLL2, in three patients with Kabuki syndrome. Am. J. Hum. Genet. 90, 119-124. doi:10.1016/j.ajhg.2011.11.021
- Lee, T. W. and Katz, D. J. (2020). Hansel, Gretel, and the consequences of failing to remove histone methylation breadcrumbs. *Trends Genet.* 36, 160-176. doi:10. 1016/j.tig.2019.12.004
- Lev, I., Seroussi, U., Gingold, H., Bril, R., Anava, S. and Rechavi, O. (2017).
  MET-2-dependent H3K9 methylation suppresses transgenerational small RNA inheritance. Curr. Biol. 27, 1138-1147. doi:10.1016/j.cub.2017.03.008
- Liao, Y., Smyth, G. K. and Shi, W. (2014). featureCounts: an efficient general purpose program for assigning sequence reads to genomic features. *Bioinformatics* 30, 923-930. doi:10.1093/bioinformatics/btt656
- Love, M. I., Huber, W. and Anders, S. (2014). Moderated estimation of fold change and dispersion for RNA-seq data with DESeq2. *Genome Biol.* **15**, 550. doi:10. 1186/s13059-014-0550-8
- Maduro, M. F. (2010). Cell fate specification in the C. elegans embryo. Dev. Dyn. 239, 1315-1329. doi:10.1002/dvdy.22233
- McMurchy, A. N., Stempor, P., Gaarenstroom, T., Wysolmerski, B., Dong, Y., Aussianikava, D., Appert, A., Huang, N., Kolasinska-Zwierz, P., Sapetschnig, A. et al. (2017). A team of heterochromatin factors collaborates with small RNA pathways to combat repetitive elements and germline stress. *Elife* 6, 7931. doi:10. 7554/eLife.21666
- Mello, C. C., Draper, B. W., Krause, M., Weintraub, H. and Priess, J. R. (1992).
  The pie-1 and mex-1 genes and maternal control of blastomere identity in early C. elegans embryos. Cell 70, 163-176. doi:10.1016/0092-8674(92)90542-k
- Morgan, M. A. J. and Shilatifard, A. (2020). Reevaluating the roles of histone-modifying enzymes and their associated chromatin modifications in transcriptional regulation. *Nat. Genet.* 52, 1271-1281. doi:10.1038/s41588-020-00736-4
- Nottke, A. C., Beese-Sims, S. E., Pantalena, L. F., Reinke, V., Shi, Y. and Colaiácovo, M. P. (2011). SPR-5 is a histone H3K4 demethylase with a role in meiotic double-strand break repair. *Proc. Natl. Acad. Sci. USA* 108, 12805-12810. doi:10.1073/pnas.1102298108
- Öst, A., Lempradl, A., Casas, E., Weigert, M., Tiko, T., Deniz, M., Pantano, L., Boenisch, U., Itskov, P. M., Stoeckius, M. et al. (2014). Paternal diet defines offspring chromatin state and intergenerational obesity. *Cell* 159, 1352-1364. doi:10.1016/i.cell.2014.11.005
- Petrella, L. N., Wang, W., Spike, C. A., Rechtsteiner, A., Reinke, V. and Strome, S. (2011). synMuv B proteins antagonize germline fate in the intestine and ensure C. elegans survival. *Development* 138, 1069-1079. doi:10.1242/dev.059501
- Quinlan, A. R. and Hall, I. M. (2010). BEDTools: a flexible suite of utilities for comparing genomic features. *Bioinformatics* 26, 841-842. doi:10.1093/ bioinformatics/btq033
- Raj, A. and Tyagi, S. (2010). Detection of individual endogenous RNA transcripts in situ using multiple singly labeled probes. *Meth. Enzymol.* 472, 365-386. doi:10. 1016/S0076-6879(10)72004-8
- Ramírez, F., Ryan, D. P., Grüning, B., Bhardwaj, V., Kilpert, F., Richter, A. S., Heyne, S., Dündar, F. and Manke, T. (2016). deepTools2: a next generation web server for deep-sequencing data analysis. *Nucleic Acids Res.* 44, W160-W165. doi:10.1093/nar/gkw257
- Rayasam, G. V., Wendling, O., Angrand, P.-O., Mark, M., Niederreither, K., Song, L., Lerouge, T., Hager, G. L., Chambon, P. and Losson, R. (2003). NSD1 is essential for early post-implantation development and has a catalytically active SET domain. *EMBO J.* 22, 3153-3163. doi:10.1093/emboj/cdg288
- Rechtsteiner, A., Ercan, S., Takasaki, T., Phippen, T. M., Egelhofer, T. A., Wang, W., Kimura, H., Lieb, J. D. and Strome, S. (2010). The histone H3K36 methyltransferase MES-4 acts epigenetically to transmit the memory of germline gene expression to progeny. *PLoS Genet.* 6, e1001091. doi:10.1371/journal.pgen.1001091
- Rechtsteiner, A., Costello, M. E., Egelhofer, T. A., Garrigues, J. M., Strome, S. and Petrella, L. N. (2019). Repression of germline genes in caenorhabditis elegans somatic tissues by H3K9 dimethylation of their promoters. *Genetics* 212, 125-140. doi:10.1534/genetics.118.301878
- Seydoux, G., Mello, C. C., Pettitt, J., Wood, W. B., Priess, J. R. and Fire, A. (1996). Repression of gene expression in the embryonic germ lineage of C. elegans. *Nature* **382**, 713-716. doi:10.1038/382713a0
- Shi, Y., Lan, F., Matson, C., Mulligan, P., Whetstine, J. R., Cole, P. A., Casero, R. A. and Shi, Y. (2004). Histone demethylation mediated by the nuclear amine oxidase homolog LSD1. Cell 119, 941-953. doi:10.1016/j.cell.2004.12.012
- Shi, Y.-J., Matson, C., Lan, F., Iwase, S., Baba, T. and Shi, Y. (2005). Regulation of LSD1 histone demethylase activity by its associated factors. *Mol. Cell* 19, 857-864. doi:10.1016/j.molcel.2005.08.027

- Sijen, T., Fleenor, J., Simmer, F., Thijssen, K. L., Parrish, S., Timmons, L., Plasterk, R. H. and Fire, A. (2001). On the role of RNA amplification in dsRNA-triggered gene silencing. *Cell* **107**, 465-476. doi:10.1016/s0092-8674(01)00576-1
- Siklenka, K., Erkek, S., Godmann, M., Lambrot, R., McGraw, S., Lafleur, C., Cohen, T., Xia, J., Suderman, M., Hallett, M. et al. (2015). Disruption of histone methylation in developing sperm impairs offspring health transgenerationally. *Science* 350, aab2006. doi:10.1126/science.aab2006
- Strome, S. (2005). Specification of the germ line. WormBook 1-10. doi:10.1895/wormbook.1.9.1
- Sulston, J. E., Schierenberg, E., White, J. G. and Thomson, J. N. (1983). The embryonic cell lineage of the nematode Caenorhabditis elegans. *Dev. Biol.* 100, 64-119. doi:10.1016/0012-1606(83)90201-4
- Tabuchi, T. M., Rechtsteiner, A., Jeffers, T. E., Egelhofer, T. A., Murphy, C. T. and Strome, S. (2018). Caenorhabditis elegans sperm carry a histone-based epigenetic memory of both spermatogenesis and oogenesis. *Nat. Commun.* 9, 4310. doi:10.1038/s41467-018-06236-8
- Tijsterman, M., Okihara, K. L., Thijssen, K. and Plasterk, R. H.A. (2002). PPW-1, a PAZ/PIWI protein required for efficient germline RNAi, is defective in a natural isolate of C. elegans. *Curr. Biol.* **12**, 1535-1540. doi:10.1016/s0960-9822(02)01110-7
- Tunovic, S., Barkovich, J., Sherr, E. H. and Slavotinek, A. M. (2014). De novo ANKRD11 and KDM1A gene mutations in a male with features of KBG syndrome

- and Kabuki syndrome. *Am. J. Med. Genet. A* **164A**, 1744-1749. doi:10.1002/ajmg.a.36450
- Unhavaithaya, Y., Shin, T. H., Miliaras, N., Lee, J., Oyama, T. and Mello, C. C. (2002). MEP-1 and a homolog of the NURD complex component Mi-2 act together to maintain germline-soma distinctions in C. elegans. *Cell* 111, 991-1002. doi:10. 1016/S0092-8674(02)01202-3
- Wang, D., Kennedy, S., Conte, D., Kim, J. K., Gabel, H. W., Kamath, R. S., Mello, C. C. and Ruvkun, G. (2005). Somatic misexpression of germline P granules and enhanced RNA interference in retinoblastoma pathway mutants. *Nature* 436, 593-597. doi:10.1038/nature04010
- Wasson, J. A., Simon, A. K., Myrick, D. A., Wolf, G., Driscoll, S., Pfaff, S. L., Macfarlan, T. S. and Katz, D. J. (2016). Maternally provided LSD1/KDM1A enables the maternal-to-zygotic transition and prevents defects that manifest postnatally. *Elife* 5, 296. doi:10.7554/eLife.08848
- Wingett, S. W. and Andrews, S. (2018). FastQ Screen: A tool for multi-genome mapping and quality control. *F1000Res* **7**, 1338. doi:10.12688/f1000research. 15931.2
- Zhang, Y., Liu, T., Meyer, C. A., Eeckhoute, J., Johnson, D. S., Bernstein, B. E., Nusbaum, C., Myers, R. M., Brown, M., Li, W. et al. (2008). Model-based analysis of ChIP-Seq (MACS). *Genome Biol.* 9, R137. doi:10.1186/gb-2008-9-9-r137